Available online at www.sciencedirect.com
ScienceDirect
Earth-Science Reviews 87 (2008) 113–133
EARTH-SCIENCE REVIEWS
www.elsevier.com/locate/earscirev

Compilation and time-series analysis of a marine carbonate $\delta^{18}O$, $\delta^{13}C$, $^{87}Sr/^{86}Sr$ and $\delta^{34}S$ database through Earth history

A. Prokoph [a,*], G.A. Shields [b,d,1,2], J. Veizer [c,3]

[a] SPEEDSTAT, 19 Langstrom Crescent, Ottawa, ON, Canada K1G 5J5
[b] Geologisch-Paläontologisches Institut, Westfälische Wilhelms-Universität Münster, Corrensstrasse 24, D-48149, Münster, Germany
[c] Department of Earth Sciences and Ottawa-Carleton Geoscience Centre, University of Ottawa, Ottawa, ON, Canada K1N 6N5
[d] Department of Earth Sciences University College London, Gower Street, London WC1E 6BT, UK

Received 21 February 2007; accepted 20 December 2007
Available online 18 January 2008

Abstract

The Sr, S, O and C isotope database of marine carbonates contains over 55,000 published isotope values of low-Mg calcite from diagenetically little altered Phanerozoic fossil shells as well as samples of whole rocks and calcite cements of Ordovician to Archean age. Carbon and oxygen isotope data for the shell material are divided into habitat subsets (high-, mid-, low-latitude and deep sea), and whole rock data are separated by mineralogy into calcite/dolomite subsets. Trend, correlation, wavelet, and spectral analyses on Gaussian-filtered isotope records were applied to detect and quantify similarities and patterns in temporal records with the following results:

(1) Oxygen isotope trends from the "high-latitude" and "deep-sea" habitats are almost indistinguishable through the last 115 Ma, consistent with the existence of the "oceanic conveyor belt" throughout this interval;
(2) All oxygen isotope habitat records show a strong, coherent 30–45 Ma (~38 Ma) cyclicity throughout the Cretaceous and the Cenozoic
(3) Up to 70% of the multi-million year variability in the $\delta^{18}O$ record of the last 115 Ma can be simulated by the following equation:

$$\delta^{18}O(‰) = 0.6\sin(2\pi t/120\ \text{Ma} + 0.9) + X\sin(2\pi t/38.3\ \text{Ma} + 1.1)$$

with X ranging from 0.4–0.6‰ for the "low-", "high-latitude" and "deep-sea" habitats, to 0.8‰ for the "mid-latitude" realm.

(1) A ~120±20 Ma cycle occurs in the Paleozoic and Neoproterozoic $\delta^{18}O$ record, consistent with paleoclimate variability as interpreted from sedimentological and faunal records.
(2) The offset of $\delta^{13}C$ values between "deep water" and "high-latitude" vs. surficial habitats at lower latitudes is consistent with the operation of a biological pump in the oceans since at least the Cretaceous.
(3) Sr and S isotope records exhibit a ~60–70 Ma cyclicity throughout the Phanerozoic.
© 2008 Elsevier B.V. All rights reserved.

Keywords: isotopes; databases; oxygen; carbon; strontium; sulfur

1. Introduction

Over recent decades some hundred thousand isotope analyses of C, O, S, and Sr have been carried out for geologic studies. Their purposes varied, as did the rock and fossil material used, the accuracy and resolution of the stratigraphy, and the care taken during sample selection. Commencing with Keith and Weber (1964) and Veizer and Compston (1974) and Veizer and Hoefs (1976), several such isotope databases have been compiled in an attempt to reconstruct global multi-million-year records of

* Corresponding author. Tel.: +1 613 247 1072; fax: +1 613 520 5613.
E-mail addresses: aprokocon@aol.com (A. Prokoph), gshields@uni-muenster.de, g.shields@ucl.ac.uk (G.A. Shields), jveizer@uottawa.ca (J. Veizer).
[1] Tel.: +49 251 83 33937; fax: +49 251 83 38312.
[2] Tel.: +44 20 7679 2363; fax: +44 20 7679 2433.
[3] Tel.: +1 613 562 5800x6461; fax: +1 613 562 5192.

0012-8252/$ - see front matter © 2008 Elsevier B.V. All rights reserved.
doi:10.1016/j.earscirev.2007.12.003

seawater isotope variability. At that time, the primary challenge was to detect and overcome diagenetic alteration of original isotope signals as well as advancing the limits of analytical precision. Subsequently, in order to avoid as much as possible the problems of diagenesis, effort has been mainly concentrated on unaltered low-Mg calcite shell material, preferably from articulate brachiopods, belemnites and foraminifera (e.g. Veizer et al., 1999; Lisiecki and Raymo, 2005). More recently, the oxygen isotope ratios of phosphatic shells of conodonts or fish teeth enamel, and of aragonitic shells (e.g. ammonites), have also been used as paleoenvironmental tracers (e.g., Picard et al., 1998).

The Phanerozoic marine $^{87}Sr/^{86}Sr$ trend has remained without significant change for about three decades because this ratio is relatively insensitive to habitat variability or to the fossil material used (Veizer et al., 1999). In contrast, oxygen and carbon isotope ratios are highly sensitive to environmental and biological factors. For example, the application of oxygen isotopes to the reconstruction of seawater temperature has to concern itself with water depth, salinity, pH and the mode of shell growth. Moreover, the species-specific physiological ("vital") factors may reflect additional variables, such as coral photosymbiosis with algae that, in turn, can modify the isotope fractionation of carbon (Abramovitch et al., 2003). As a consequence, with an improved understanding of isotopic proxies for reconstruction of past environments, there has emerged a need to address not only the temporal variability of the signal but also the variability due to habitat and organism-specific isotope fractionation parameters (e.g., Spero and DeNiro, 1987).

In this review, we constructed separate Phanerozoic oxygen and carbon isotope records for "deep water" and for "high-", "mid-" and "low-latitude" surface water in an attempt to improve the reconstruction of paleoenvironmental conditions. We calibrated these datasets to an articulate brachiopod standard, in order to address the differences in habitat and physiology of the organisms. Brachiopods were chosen as a standard because they have been extant since the Cambrian and, except for the Cenozoic, the bulk of Phanerozoic O and C isotope measurements were carried out on their shells. The Precambrian records are based on calcitic or dolomitic components of whole rock carbonate samples.

The aims of this review are:

(1) to provide the scientific community with an updated (up to February 2006) compilation of marine Sr, O, C, and S isotope data from published literature for the entire Earth history. The database is fully annotated, grouped into different habitats where deemed necessary, and consistently referenced to the new geologic time-scale GTS2004 (Gradstein et al., 2004);
The storage of the database in a secure databank where it can be available to the community for their own retrieval and manipulation is the primary goal of this publication, because with Veizer's retirement, its continuation and even survival cannot be guaranteed. The supplementary goals listed below are only tentative suggestions for future advances in development and interpolation of the database.
(2) to carry out data processing that transforms the raw data into habitat-specific geologic records;
(3) to determine long-term trends, periodic patterns and interrelationships within and between the isotope records using time-series analytical techniques;
(4) to interpret the results of the time-series analysis in terms of paleoenvironmental reconstructions.

We particularly avoided any reconstruction of records through time intervals where no data are available. Differences in temporal data density are clearly highlighted. In this way, the reader can easily recognize for which time interval and at which resolution the suggested reconstructions and interpretations are robust or less so. All raw data used for record compilations associated with this article can be found at doi:10.1016/j.earscirev.2007.12.003.

2. Phanerozoic fossil data

2.1. Data selection

This review is an update and restructuring of the Ottawa–Bochum O, C, S and Sr isotope database for marine carbonates (Veizer et al., 1999; Shields and Veizer, 2002; Kampschulte and Strauss, 2004). The updated database includes oxygen and carbon isotope data for fossil shells from 146 references, three references for sulfur isotope values from marine sulfates, and 43 references for strontium isotope ratios of fossil shells and micrite. In order to extend the fossil carbonate database to cover the entire Phanerozoic, it has been supplemented by Cambrian whole rock carbonate data (11 references for $^{87}Sr/^{86}Sr$ and 16 for $\delta^{18}O$ and $\delta^{13}C$).

The database includes over 39,000 $\delta^{18}O$ and $\delta^{13}C$ values for the low-Mg calcite or aragonite of diagenetically little altered shells of ammonites, belemnites, brachiopods, inoceramids, trilobites, benthic and planktonic foraminifera, as well as micrite and conodont data for $^{87}Sr/^{86}Sr$ (Table 1). The 380 $\delta^{34}S_{sulfate}$ data are from marine barites and structurally substituted sulfate. A set of 2282 whole rock samples, mostly deriving from references up to 2002, has been included to fill the large stratigraphic gaps between shell samples in the Cambrian. For consistency, the deep-sea carbon and oxygen isotope data of the last 67 Ma were taken entirely from the benthic foraminifera dataset of Zachos et al. (2001). Isotope data for shell material with Mn concentrations >350 ppm, some duplicate data entries, and Holocene foraminifera data from the Ottawa–Bochum database (Veizer et al., 1999) have not been incorporated into the new database. In addition, the abundant Quaternary isotope data from the literature have not been utilized in this database. The only exceptions are the articulate brachiopod data because of their importance as a standard for the Phanerozoic isotope records.

The individual samples of the database represent discrete measurements that are subject to stratigraphic uncertainty as well as errors in both analytical and palaeoenvironmental interpretations. All sample ages were transformed from their original time scale into the GTS2004 time scale (Gradstein et. al., 2004) and include also estimates of the $\pm 1\sigma$ stratigraphic uncertainty.

Table 1
Seawater isotope database

Material/fossil	All	All	Low-latitude		Mid-latitude		High-latitude		Deep sea		Miscellaneous		All	Veizer et. al. (1999)
	Sr	34S	C	O	C	O	C	O	C	O	C	O	C/O	C/O
Belemnites	435		150	164	962	975	69	73						628
Planktic foraminifera	1666		602	766	489	493	109	163			136	115		76
Brachiopods	1235		3794	3889	99	101	9	11				4		3733
Benthic foraminifera (deep sea)									9763	11175	9	9		680[#]
Benthic foraminifera (neritic)											17	17		
Trilobites			4	4										
Inoceramids	7										61	61		
Bivalves											50	50		1
Oysters	63										102	125		119
Ammonites											58	58		
Bivalve larvas											5	5		
Echinoderms											3	3		
Gastropods											8	8		
Corals	11										3	3		2
Conodonts	623													
Micritic carbonate	186													
Total: fossils	4226	0	4550	4823	1550	1569	187	247	9763	11175	452	458	16503/18277	4559
Structurally substituted sulfate		225												
Barite		155												
Whole rock	1355	68	7872	7222										
Total	5581	448	12422	12045	1550	1569	187	247	9763	11175	452	458	16503/18277	4559

[#] Portion of Veizer et al. (1999) database not included in this database.

Samples with a cumulative stratigraphic uncertainty >5% of the mean sample age were excluded from the database. All these uncertainties were assessed very conservatively for cases where no detailed stratigraphy or age has been provided. A minimum 1σ uncertainty of 0.5% of the mean age has been applied to all samples, even if the original source stated a narrower age uncertainty. Nevertheless, the assignment of accurate stratigraphic mean ages and uncertainties is often problematic and will certainly change with updated time scales and radioactive decay constants.

2.2. Oxygen and carbon isotope data

The Phanerozoic database includes information on timescale, stratigraphic uncertainty, sample age, fossil groups, habitat, literature source, sample location and other comments. The database is organized as an MS EXCEL spreadsheet with sheets for different habitats and a miscellaneous category.

The updated carbon and oxygen database has been structured according to the following habitat designations:

(1) surface waters between 58°–90° paleolatitudes ("high-latitude"),
(2) surface waters between 32°–58° paleolatitudes ("mid-latitude"),
(3) surface water between 32°N and 32°S paleolatitudes ("low-latitude"),
(4) "deep sea" below 300 m water depth.

We recognize that this division is somewhat arbitrary because the extent of paleogeographic zones will vary with climates of greenhouse/icehouse types. Nevertheless, with the present-day state of the art, any further specification would have to be speculative.

The surface water habitats (1–3) do not exactly follow the polar circles and tropics for the following reasons:

(1) Paleogeographic reconstructions of the Paleozoic are not known well enough for delineation of exact climate realms. In this study, the widening of the tropics to 32° latitude allows us to accommodate almost all pre-Jurassic fossil data into the "low-latitude" category, an assignment more reflective of their habitat. The Cretaceous planktic foraminifera from latitudes ~25–32° are also more representative of a tropical than of a temperate climate (Huber et al., 1995).

(2) Samples from latitudes 58–60°, as a group, have significantly heavier $\delta^{18}O$ values than other "mid-latitude" samples.

Most of the belemnite and planktic foraminifera data of the Ottawa–Bochum database (Veizer et al., 1999) are now part of the "mid-latitude" realm subset, and most of their brachiopod samples part of the "low-latitude" realm subset, respectively. In order to avoid local geographic bias on the global perspective of this study, data from sections that were sampled at very high stratigraphic resolution were down-sampled by including only ~20 kA averages.

The database also includes a fifth category ("*Miscellaneous*") for data that do not fulfill our requirements for compiling a consistent isotope record. Samples included into this group are:

(1) Fossils with aragonite shells, for example ammonites.
(2) Fossils that cannot be assigned reliably to surface water above the thermocline or to the deep sea, such as the thermocline/subthermocline planktic foraminifera (e.g., Rotaliporae, Subbotinea) or the shallow water benthic foraminifera.
(3) Samples from epicontinental seas or marine basins with restricted water exchange with the open ocean, such as the Mediterranean Sea during the late Miocene (i.e. the Messinian Crisis) or the Western Interior Seaway of North America. Most data from these environments are not retained in the database.
(4) Samples exhibiting probable isotopic disequilibrium between seawater and shell (i.e. "vital effects"). For example, the planktic foraminifera with high $\delta^{13}C$ isotope values that likely lived in photosymbiosis with algae.
(5) Fossil groups of inoceramids, bivalves, corals, as well as unaltered surface dwelling tropical planktic foraminifera (e.g., Pearson et al., 2001) because, at this stage, they could not be calibrated to the brachiopod standard.
(6) Paleozoic samples with $\delta^{18}O$ of less than −14‰, because they are almost certainly diagenetically altered. These samples were also excluded from data analyses and interpretations by Veizer et al. (1999) and subsequent publications.

Data from the "*Miscellaneous*" category are not included in any plots and data analysis, but have not been discarded as they may become useful once more information and related metadata have been collected. Many of these fossil groups have already been shown to serve as useful paleoenvironmental proxies for high-resolution and regional studies (e.g., Picard et al., 1998; Dromart et al., 2003; Zakharov et al., 2001).

Insufficient stratigraphic range and density of data within each fossil group generates some problems with habitat assignment. Among the sampled fossils, brachiopods have the longest stratigraphic range, and they have been studied for vital and diagenetic effects. In addition, they represent the largest shallow water dataset for the "low-latitude" habitat. In this study, they therefore provide the baseline to which all other fossil groups are calibrated. The details of the calibration are outlined in Section 4.2.

In summary, only brachiopods, belemnites, trilobites, and planktic foraminifera are included in categories (1) to (4) above. Whole rock data have been added to cover the otherwise stratigraphically incomplete Cambrian fossil dataset for the "low-latitude" realm (Fig. 1). The "mid-latitude", "high-

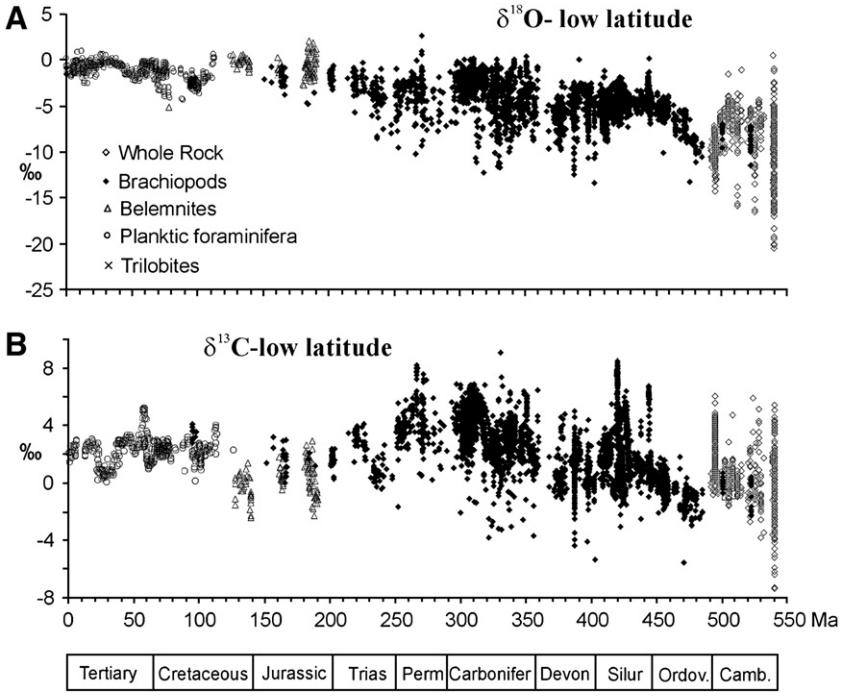

Fig. 1. Raw $\delta^{18}O$ (A) and $\delta^{13}C$ (B) data from the "low-latitude" realm for the last 543 Ma. Time-scale GTS2004 (Gradstein et al., 2004).

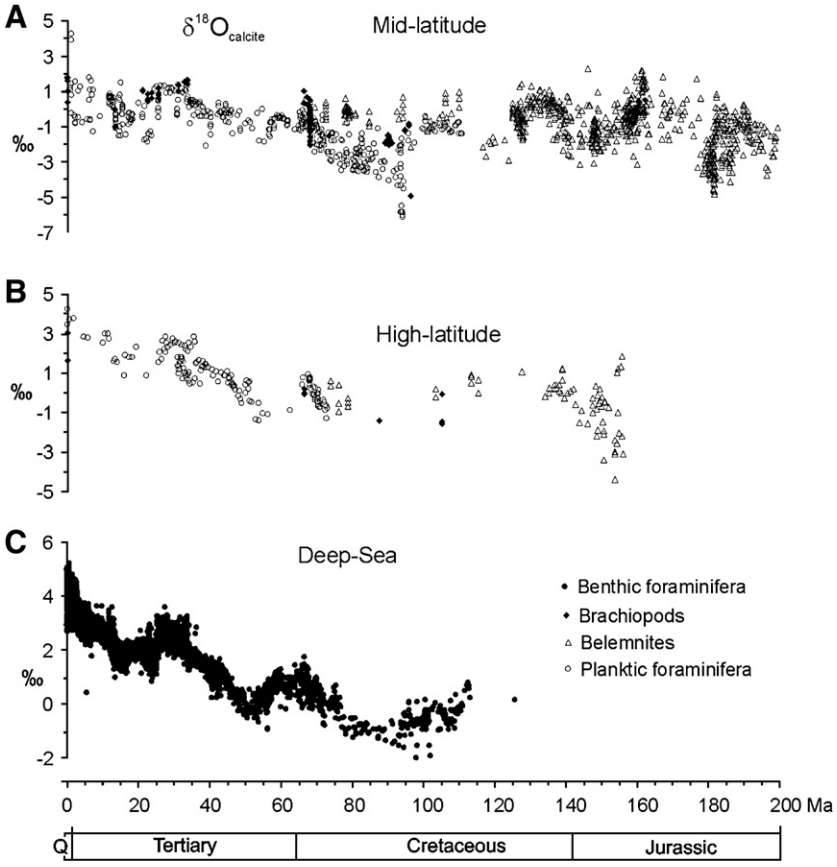

Fig. 2. Raw $\delta^{18}O$ data for the "mid-latitudes" (A), "high-latitude" (B) and "deep-sea" (C) categories for the last 200 Ma. Time-scale GTS2004 (Gradstein et al., 2004).

latitude" and "deep-sea" oxygen isotope subsets have no data entries older than 200 Ma, 156 Ma and 126 Ma, respectively (Fig. 2). The carbon isotope data for the "mid-latitude", "high-latitude" and "deep-sea" habitats are generally from the same sample populations as the oxygen isotope data. "High-latitude" carbon isotope data are, however, sparse (Fig. 3).

2.3. Strontium isotope data

The entire Phanerozoic $^{87}Sr/^{86}Sr$ database of marine carbonates is composed of 4226 samples from diagenetically unaltered or demonstrably little altered low-Mg calcite shell material of brachiopods, belemnites, corals, inoceramids, planktic foraminifera, oysters, micritic carbonate (mostly nanoplankton), as well as from apparently well preserved conodont apatite (Table 1). These data are complemented by 400 whole rock samples that fill stratigraphic gaps in the fossil data (Fig. 4).

The $^{87}Sr/^{86}Sr$ database is organized into three subsets ("fossil", "omitted", and "whole rock"). Omitted data have insufficient quality (e.g. diagenetic alteration) or missing essential information on the sample (e.g., precise location and age). The "fossil" and "omitted" subbase includes data on age, stratigraphic uncertainty, sample age, data source, fossil group, and location. All measured $^{87}Sr/^{86}Sr$ values are normalized to NBS 987 of 0.710250. The whole rock subset is organized for consistency with the PMCID 1.1. database (Shields and Veizer, 2002), which is the only source of these data.

It is not necessary to classify samples into "habitat" subsets as the strontium isotope ratio of marine carbonate is habitat and physiology independent; moreover the world's oceans are well mixed with respect to $^{87}Sr/^{86}Sr$ (Peterman et al., 1971; Veizer and Compston, 1974; McArthur et al., 2000).

2.4. Sulfur isotope data of marine sulfate

The $\delta^{34}S$ database of seawater sulfate is composed of 380 barite or structurally substituted sulfate samples from three literature references (Table 1, Fig. 5), and is organized into three subsets ("fossil", "omitted", and "whole rock") with information on sample age (in GTS2004), stratigraphic uncertainty, $\delta^{34}S$ sample, and literature reference.

There is no known habitat related bias to the $\delta^{34}S$ ratio of seawater sulfate in unrestricted marine environments, and no subsets were therefore generated.

3. Precambrian whole rock data

The majority of data utilized in this database was compiled previously in the Precambrian marine carbonate isotope database: Version 1.1 of Shields and Veizer (2002). We have added literature data from 2001–2006, with particular emphasis on the Neoproterozoic (Jaffrés, 2005; Jaffrés et al., 2007) and the Archean.

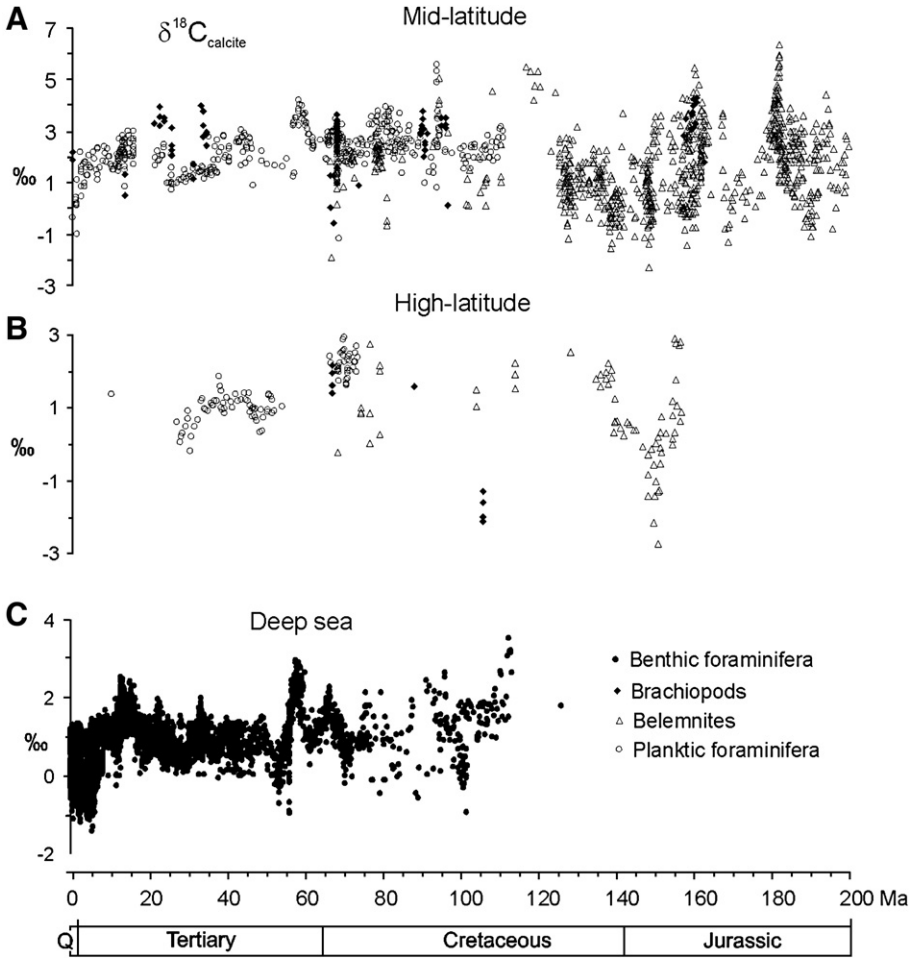

Fig. 3. Raw $\delta^{13}C$ data from the "mid-latitudes" (A), "high-latitude" (B) and "deep sea" (C) for the last 200 Ma. Time-scale GTS2004 (Gradstein et al., 2004).

For the Precambrian compilation, we selected isotope values according to the following criteria:

(1) The samples are believed to be of marine origin;
(2) Oxygen and carbon isotope samples are from carbonate rocks of calcitic or dolomitic mineralogy only;
(3) Mean sample ages can be assigned with a 95% confidence within a 100 Ma ($\pm 1\sigma = 50$ Ma) bracket.

Based on these criteria, we compiled Precambrian and early Paleozoic whole rock isotope data for $\delta^{18}O_{calcite}$ ($n=3334$), $\delta^{18}O_{dolomite}$($n=3898$), $\delta^{13}C_{calcite}$($n=3467$), $\delta^{13}C_{dolomite}$($n=4405$)

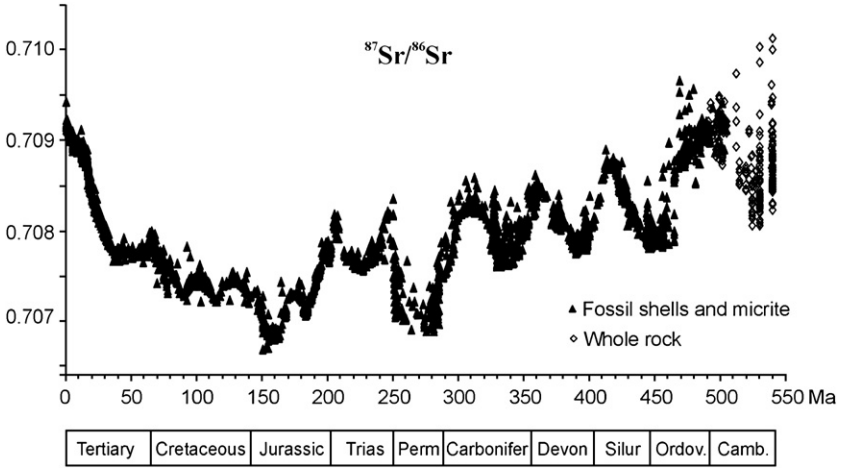

Fig. 4. Raw $^{87}Sr/^{86}Sr$ data for the last 543 Ma. Time-scale GTS2004 (Gradstein et al., 2004).

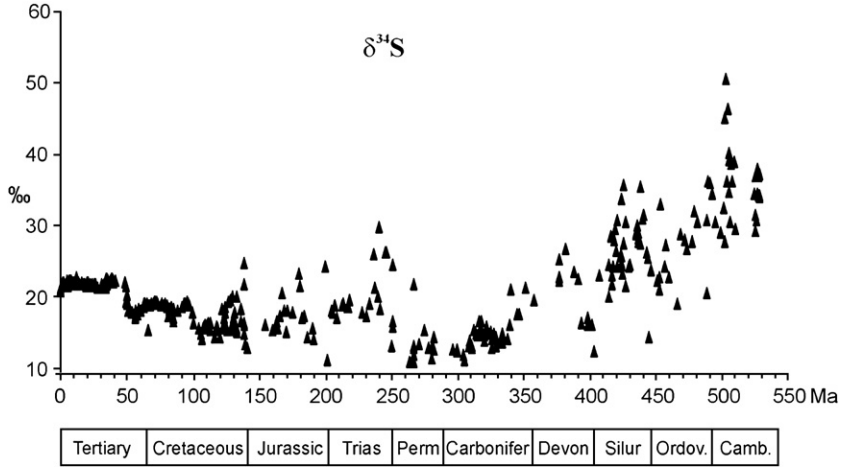

Fig. 5. Raw $\delta^{34}S$ data from structurally substituted sulfur and barite for the last 543 Ma. Time-scale GTS2004 (Gradstein et al., 2004).

and $^{87}Sr/^{86}Sr$ ($n=1355$). Precambrian $\delta^{34}S_{sulfate}$ data are as yet too sparse to yield a statistically robust record. Only the isotope records of mineral phases that may reflect more or less directly the isotopic composition of seawater are discussed here. Complementary databases, such as the $\delta^{34}S_{sulfide}$ or $\delta^{13}C_{org}$ are not included in this review. Readers are referred to other publications such as Strauss et al. (1992), Canfield and Raiswell (1999) and Strauss (2002) for this information.

The databases are composed of discrete measurements that have some stratigraphic uncertainty as well as superimposed uncertainties reflecting technical and environmental limitations. All sample ages have been transformed from their original time scale into the GTS2004 time scale (Gradstein et. al., 2004) using linear interpolation between system boundaries, and include estimates of the 1σ-stratigraphic uncertainty derived from the original reference. The whole rock data range in age from 445 Ma (Ordovician) to 3750 Ma (Archean).

4. Record assembly

4.1. Construction of the continuous record

The data were transformed into a continuous stratigraphic record (i.e. time series) using the Gaussian filtering method that assigns 1σ-stratigraphic uncertainty to each sample (e.g.

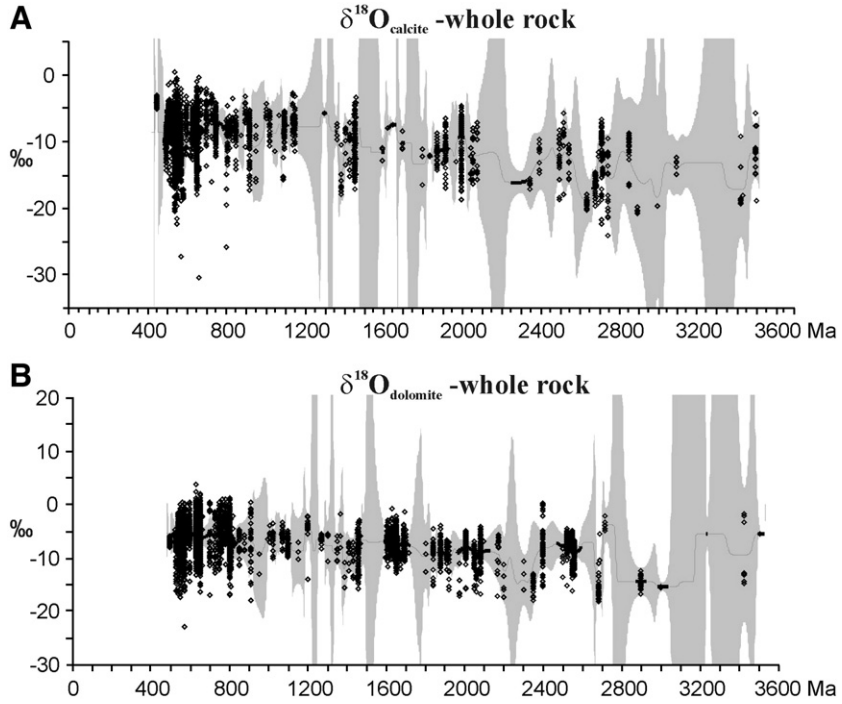

Fig. 6. Compilation of raw whole rock $\delta^{18}O$ isotope data for limestones and dolostones for the last 3800 Ma. Lines indicate the continuous Gaussian trends. Grey shaded areas mark the standard errors of the means. Note that the number of samples decreases exponentially with age.

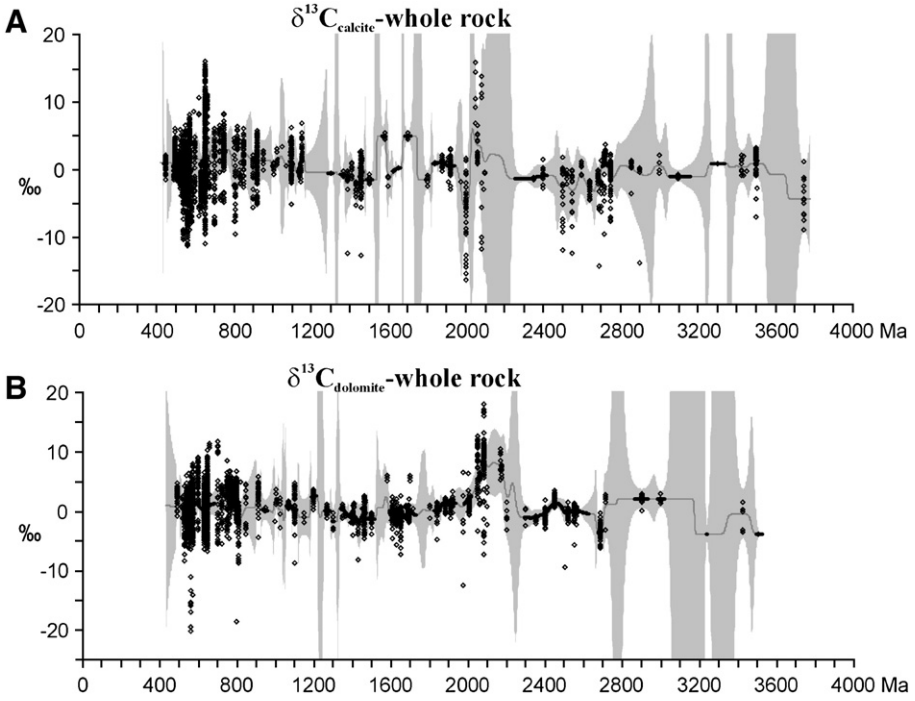

Fig. 7. Compilation of raw whole rock $\delta^{13}C$ isotope data for limestones and dolostones for the last 3800 Ma. Explanations as in Fig. 6. Note that the number of dolomite samples remains relatively high until ~2700 Ma ago.

Prokoph et al., 2004). The estimate of stratigraphic uncertainty is a cumulative of the following parameters:

(1) The radioactive decay constant of the isotopes that are primarily used for the construction of time scales (Agterberg, 1994);
(2) The reference age of the radioactive isotope used, such as the Fish Canyon Tuff for Ar–Ar-ages (Courtillot and Renne, 2003);
(3) The uncertainties of zone, system and other stratigraphic boundaries that result from time-scale models (Agterberg, 1994); and

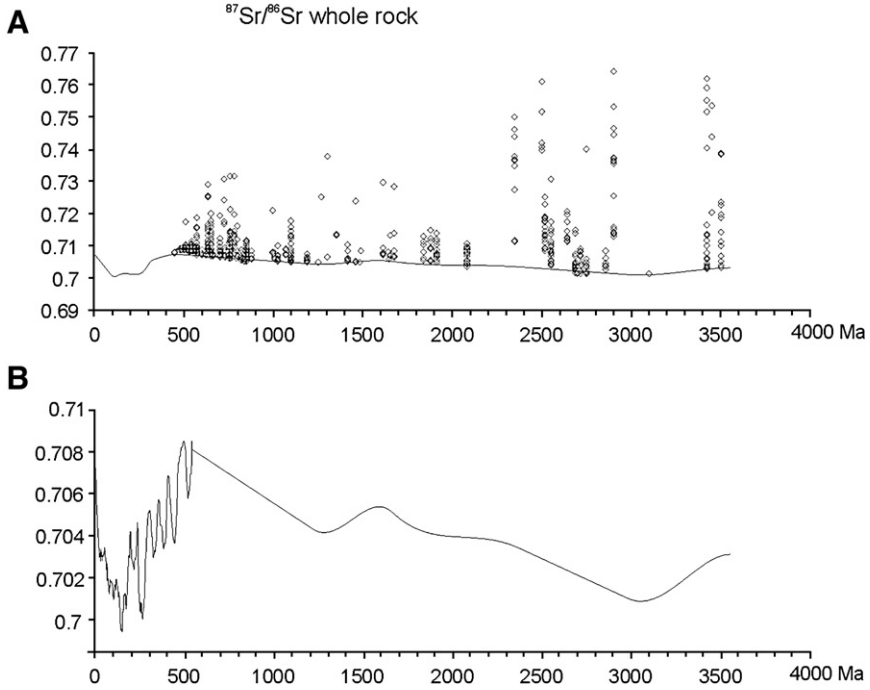

Fig. 8. Compilation of raw whole rock strontium isotope data for the last 3500 Ma (A). The secular trend is based on fossils for the Phanerozoic and on the envelope for the least radiogenic values for the Precambrian (B).

Table 2
Offsets and correction to brachiopod data

Latitude	Material/fossil	$\delta^{13}C$				$\delta^{18}O$			
		Offset mean	ε_S	n	Correction applied	Offset mean	ε_S	n	Correction applied
Low-latitude	Belemnites	1.20	0.17	8	1.20	−2.50	0.54	8	−2.50
	Planktic foraminifera	1.55	0.10	5	1.60	−0.04	0.21	6	0.00
	Trilobites	−0.15	0.47	4	−0.20	0.63	0.00	3	0.60
	Whole rock (Cambrian)	−1.41	0.22	13	−1.40	0.09	0.05	10	0.10
Mid-latitude	Belemnites	0.58	0.31	16	0.60	−0.32	0.17	16	−0.30
	Planktic foraminifera	0.55	0.28	20	0.60	0.83	0.27	20	0.80

n — number of comparite 1 Ma-time intervals with data density $p>0.3$ (brachiopods) and $p>0.25$ (other fossils).

(4) The stratigraphic width of the biozone, paleomagnetic zone, or orbital cycle used for stratigraphic refinement of the sample location.

Gaussian filtering assumes that age uncertainties are symmetrically (bell-shaped) distributed, providing for each sample an infinite and continuous distribution with infinite resolution. Thus, theoretically, Gaussian probability never reaches zero. The time series of the sum of all probabilities p forms a data density/Ma — curve. As a result, the Gaussian-filtered isotope time series represents the trend of sample averages, weighted according to the probability that they fall within a particular age interval. For each time interval i, the standard deviation "σ" is calculated from the differences between the weighted average of individual samples and the 1 Ma — mean value. The standard error $\varepsilon=\sigma_i/\sqrt{p_i}$, with p representing the age in Ma, is used as an estimate of the significance of the 1 Ma — mean value that is used for the record.

Gaussian probability functions were applied cumulatively for each sample at 1 Ma intervals for graphical data presentation. For time-series analysis, we down-scaled the records to 2.5 Ma intervals for the last 200 Ma, 5 Ma for the Triassic to Cambrian, and to 25 Ma for the entire 3500 Ma record. Thus, we should be able to detect potential patterns at 5, 10, and 50 Ma resolution, respectively. In this way we can accommodate the increasing stratigraphic uncertainty and decreasing density of data with age.

Gaussian filtering has the advantage that the stratigraphic uncertainty of each sample is preserved in the assembled record. For example, a sample with a mean age of 18.1 Ma belongs partially to the 17–18 Ma (~40%) as well as to the 18–19 Ma (~60%) interval, not 100% to the 18–19 Ma interval.

By contrast, the method applied to our earlier databases (Veizer et al., 1999, 2000; Shields and Veizer, 2002) calculates average values from all data that have mean ages falling into a specific age interval. The disadvantage of that approach is that stratigraphic uncertainty cannot be assigned, but it has the advantage that large differences in sample density for successive age intervals have no smearing effect on the record. In order to compensate for this smearing effect, for the Phanerozoic time-series analysis we retained only data with a density $p>0.25$. The outputs with $p<0.25$ were replaced by linearly interpolated values (Shackleton and Imbrie, 1990). For calculation of the Precambrian oxygen and carbon isotope trends (Figs. 6, 7) we used $p<0.1$, instead of $p<0.25$, because the smearing effect decreases for older samples due to their higher 1σ-age uncertainty. The Precambrian strontium isotope data are a special case because due to their high sensitivity to diagenetic alteration, the mean would be shifted to highly radiogenic values, and thus meaningless for any interpretation of seawater evolution. In this case, we accept only the envelope skirting the lowest measured values (Fig. 8) as the best approximation (Veizer and Compston, 1974) to the $^{87}Sr/^{86}Sr$ composition of contemporaneous seawater.

4.2. Habitat correction

The carbon and oxygen isotope signature of fossil shell carbonate is strongly dependent on the water mass in which the fossil lived and grew, as well as on physiological ("vital") effects that controlled how each taxa fractionated isotopes during shell growth (Corfield et al., 1990; Spero et al., 1997; Abramovitch et al., 2003). In order to construct a consistent isotope record it is necessary to calibrate the isotope fractionation effects and different life styles of the organisms to a common standard. Here we introduce an "articulate brachiopod standard" (ABS), because:

(1) the articulate brachiopod group has a stratigraphic range from the Cambrian to present;
(2) brachiopod habitats and their vital effects have been studied;
(3) the diagenetic alteration of the shells can be evaluated;
(4) brachiopod isotope data are known for almost the entire Phanerozoic; and

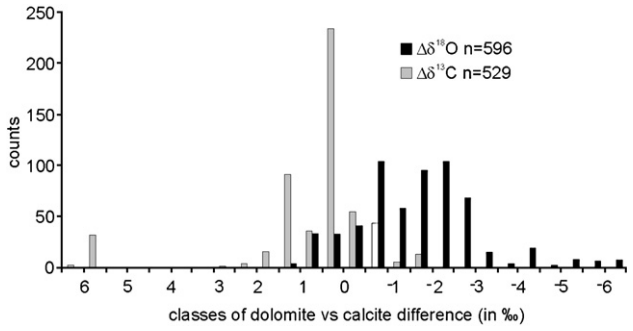

Fig. 9. Histogram showing the distribution of offsets between dolomite and calcite samples at class sizes of 0.5‰.

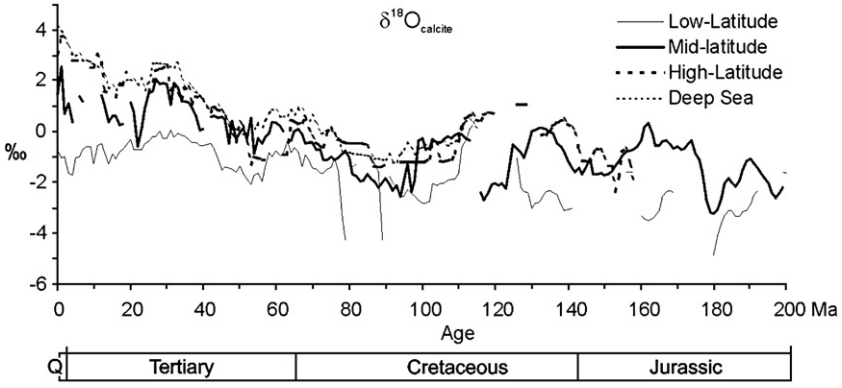

Fig. 10. Gaussian-filtered and articulate brachiopod-calibrated $\delta^{18}O$ data at 1 Ma resolution for different habitats for the last 200 Ma. Note that only data from intervals with a data density of $p>0.25$ are plotted. Time-scale GTS2004 (Gradstein et al., 2004).

(5) their primary shell material consists of low-Mg calcite for which a transfer function to water temperature can be established.

The ABS is calculated from the average offset in the isotope values between brachiopods and other fossil groups. In previous studies, the differences in $\delta^{18}O$ and $\delta^{13}C$ values between different fossil groups and habitats were observed mostly over short stratigraphic intervals (e.g. Lu and Keller, 1996; Voigt et al., 2003). In the present study, the offsets were calculated from Gaussian-filtered data at 1 Ma intervals for temporal sections where coeval data density for brachiopods attained $p>0.3$ and for other fossil groups $p>0.25$. The number of 1 Ma-time intervals depends strongly on the stratigraphic sampling resolution of the fossil groups. The standard deviation for each interval is derived from $1/n-1*\Sigma(x_i-y_{ij}*p_{ij})$ with x_i the mean value per 1 Ma time interval i, n the isotope sample size, y_{ij} the individual isotope value per sample and p_{ij} its probability of belonging to the time interval i. The standard error $s/\sqrt{p}$ of the arithmetic mean of the individual differences is used to indicate the statistical robustness of the estimated offsets.

The offsets in carbon and oxygen isotope values between fossil groups and brachiopods have been calculated for "low-", "mid-" and "high-latitude" surface waters. For the "deep-sea" record only benthic foraminifera are used and no further standardization in the absence of deep-sea brachiopods is possible. Note that the stratigraphic coverage of brachiopods is sparse for the last 200 Ma. This interval, on the other hand, is well covered by planktic foraminifera, at least for the last ~115 Ma, and by belemnites for several intervals from ~100–200 Ma. Trilobite and whole rock data are restricted to the Cambrian Period.

The offsets to brachiopod standards (ABS) utilized in this review are summarized in Table 2. The standard error of 0.54 on the −2.5‰ $\delta^{18}O$ belemnite offset is unusually high and this correction may turn out to be an overestimate. This offset is based on the study of low-latitude Jurassic sequence in Spain (Rosales et al., 2001, 2004) which contains coeval brachiopod and belemnite fauna. If correct, it may imply that belemnites grew/lived in deeper, colder water than brachiopods. The estimate of the $\delta^{13}C$ offset is much smaller and with a lower standard error. The $\delta^{18}O$ offset for planktic foraminifera is very small for "low-latitude" environments (−0.04‰), but it is

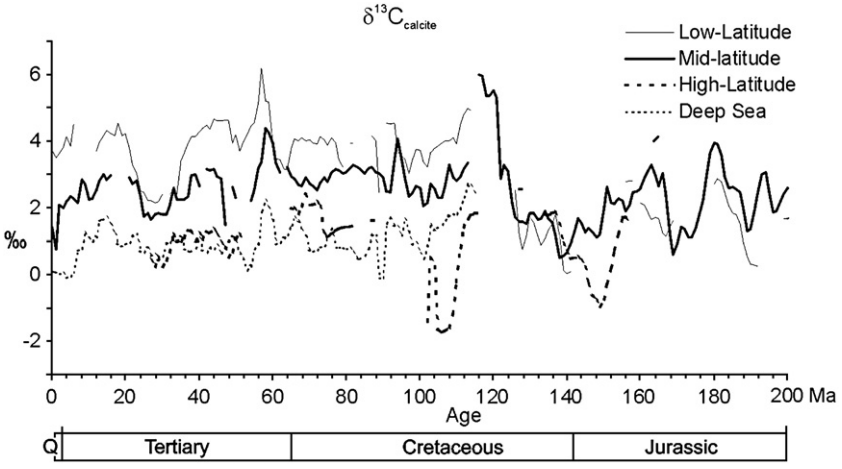

Fig. 11. Gaussian-filtered and articulate brachiopod-calibrated $\delta^{13}C$ data at 1 Ma resolution for different habitats for the last 200 Ma. Note that only data from intervals with a data density of $p>0.25$ are plotted. Time-scale GTS2004 (Gradstein et al., 2004).

significantly higher (+0.83‰) for the "mid-latitude" sets. Their $\delta^{13}C$ offsets show a reverse pattern. In general, the standard errors on the $\delta^{18}O$ and $\delta^{13}C$ offset estimates between brachiopods and planktic foraminifera are low and provide a relatively robust basis for calibration. Fossil groups assigned to the *Miscellaneous* category have insufficient data density coeval with the brachiopods for any adjustment to be contemplated.

At this point, it is not possible to calculate the offsets between brachiopods and other fossil groups in the "high-latitude" dataset because of the paucity of coeval brachiopod data (Table 2).

For whole rock samples, the small ε_s for the $\delta^{18}O$ offset indicates that these samples may yield a reasonable approximation to calcium carbonate in isotopic equilibrium with the surface ocean. The situation is less satisfactory for the $\delta^{13}C$ data (Table 2).

4.3. Rock type correction

Rock type corrections have been applied to the whole rock, mostly Precambrian, data to correct for the offset between calcite and dolomite samples. The isotope signature of a mineral phase depends on its depositional environment and subsequent diagenetic history, in addition to any mineralogy-dependent fractionations in the case of oxygen. As already discussed, strontium isotopes are almost independent of habitat. Whole rock and fossil samples have therefore almost identical values initially, but may be strongly altered by later diagenetic processes. For whole rock oxygen and carbon isotopes, the current state of the database still does not permit environmental corrections. Here we assume that the whole rock samples were all deposited in a "low-latitude", shallow marine environment. Many of these samples are known to have originated as primary precipitates, early diagenetic replacements or as early diagenetic marine cement in cavities within as microbial mats, or stromatolites, but others, such as most Archean metacarbonates, are of uncertain origin. The calcite-dolomite offsets, calculated from Gaussian-filtered data at 1 Ma interval with low uncertainty (ε_i<standard deviation of the 445–3505 Ma record), were calculated from 596 and 529 coeval pairs for oxygen and carbon isotopes, respectively.

The mean $\delta^{18}O$ offset between dolomitic and calcitic samples is −2.14‰, with a standard deviation of 1.41‰. For carbon isotope data the offset is 0.13‰ with a standard deviation of 1.50‰. Note that the carbon isotope offset is much more narrowly defined than is the case for the oxygen (Fig. 9).

While the use of whole rock samples for reconstructing the marine oxygen and carbon isotope records has its problems, Brand (2004) demonstrated that over specific time intervals they correlate well, and without offset, with brachiopod data (Ordovician), but deviations may exist (Carboniferous). Unfortunately, the absence of suitable fossils in the Cambrian obliges us to use whole rock or micrite data to fill the gaps in the $\delta^{18}O$ and $\delta^{13}C$ records.

Because the offset between Cambrian fossil and whole rock data is −0.1‰ for $\delta^{18}O$, and −1.41‰ for $\delta^{13}C$ (see above), we corrected the raw whole rock $\delta^{18}O_{calcite}$ data by −0.1‰, the $\delta^{13}C_{calcite}$ data by −1.41‰ and the $\delta^{13}C_{dolomite}$ data by −1.54‰ (=−1.41‰+−0.13‰). We did not correct the $\delta^{18}O_{dolomite}$ data and excluded them from further processing, because their large standard deviation posed a problem for linkage with the fossil and calcite data.

5. Data analysis methods

We applied several time-series analysis methods to determine and quantify major patterns in the set of isotope records. Trend, linear correlation, and linear regression analysis are applied to evaluate trends and relationships in and between the isotope sets (e.g., Davis, 1986). Spectral and wavelet analysis are used to determine, quantify, and extract periodic patterns in the records (e.g., Torrence and Compo, 1998). For data analysis, all Gaussian-filtered 1 Ma data with a density p_i<0.25 were removed because of their smearing effect (see above). For spectral analysis, the resulting gaps in the records were replaced by linearly interpolated data.

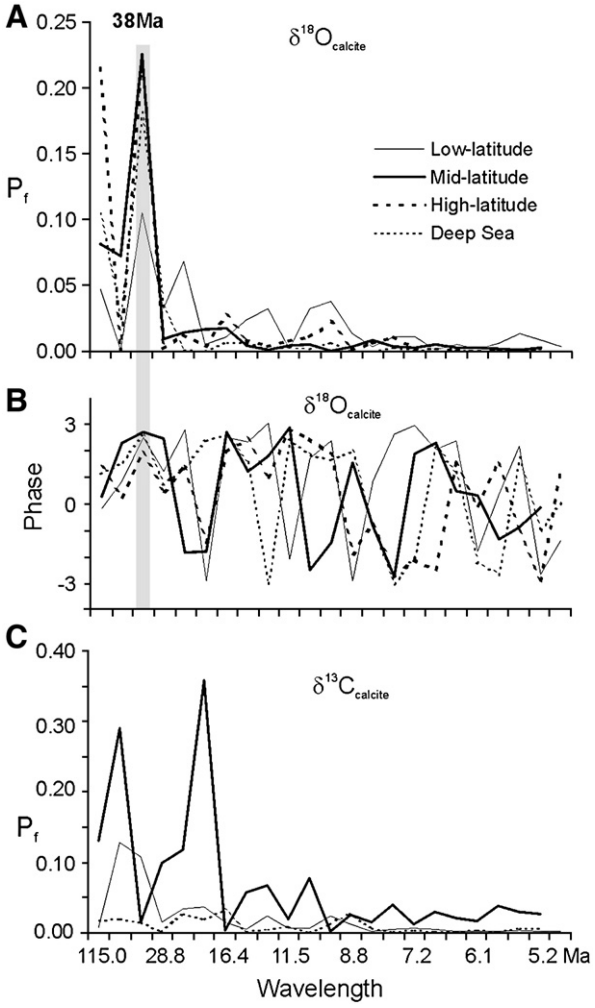

Fig. 12. Spectral analysis of the brachiopod-corrected $\delta^{18}O$ and $\delta^{13}C$ records for the last 115 Ma. Note the similarity in spectral power (A) and phase (B) of the ~38 Ma $\delta^{18}O$-cycle for all habitats. No spectral similarity exists between the different $\delta^{13}C$ habitat records (C) and phase comparison was therefore deemed unnecessary.

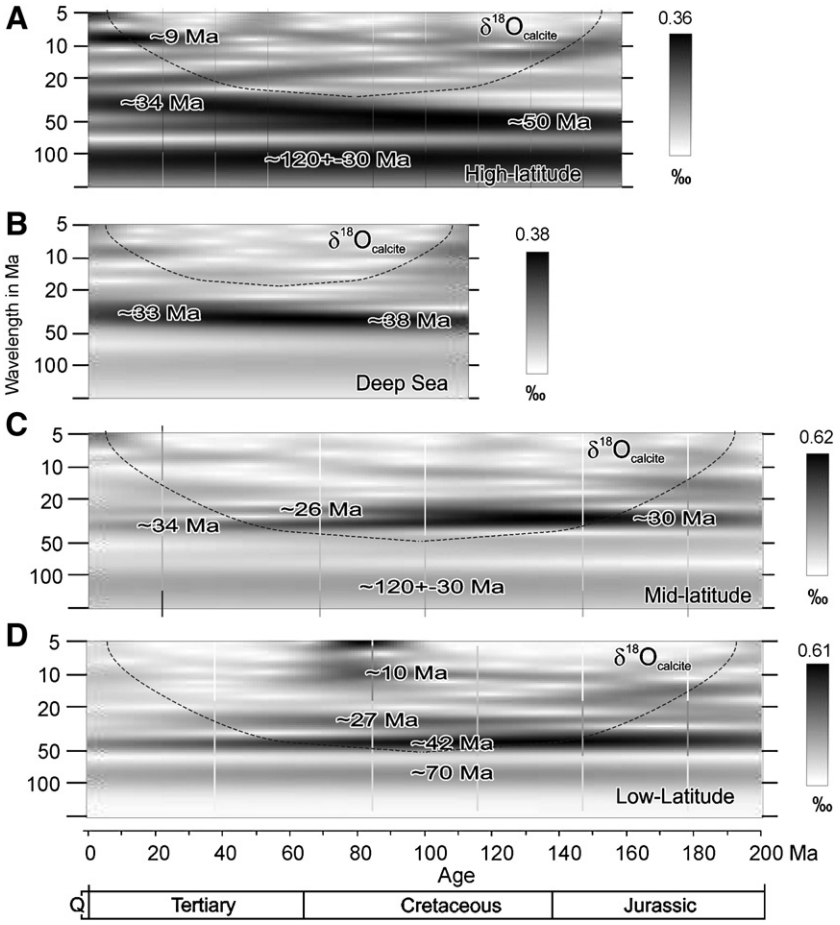

Fig. 13. Scalograms of wavelet transform for brachiopod-corrected $\delta^{18}O$ records for different habitats for the last 200 Ma. Area below dashed lines has >20% wavelet coefficient reduction due to edge effect. Right side: Grey-scale code for wavelet coefficient above zero (white). Note that all records exhibit their highest wavelet coefficients in the 20–50 Ma waveband.

Spectral analysis (Fourier transform) is defined by

$$p^2 f = \int x(t) e^{-i2\pi ft} dt \quad (1)$$

with $x(t)$ the discrete time series, f the frequency, and P^2 the spectral power (Davis, 1986). The spectral power is illustrated by its "power spectrum". There are different ways to calculate the spectral power. Here, we used the periodogram to express the spectral power, that is, the raw, squared Fourier coefficients, which allow us to calculate the signal amplitudes for further filtering or data-driven modeling purposes. Phases of each periodic signal have been extracted to determine the

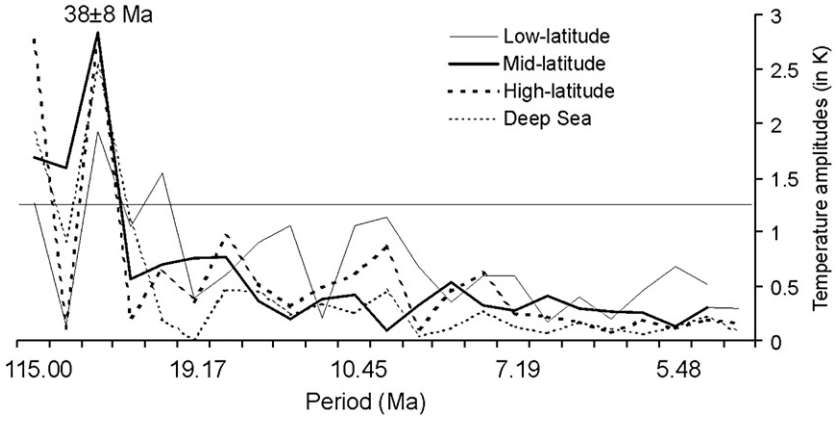

Fig. 14. Spectral analyses of the seawater temperature for different habitats derived from the brachiopod-corrected $\delta^{18}O$ records for the last 115 Ma. The horizontal solid line represents the threshold below which the $\delta^{18}O$ fluctuations can be explained as due solely to ice-sheet dynamics. The line shows the power spectrum p that would arise from a sinusoidal ‰ fluctuation converted to temperature using the transfer function of Faure (1998) with $p=((4.14*(x-0.3‰)+0.13*(x-0.3‰)^2))$ and $x=1‰$.

temporal deviation between different isotopes and different habitats.

The wavelet coefficients W of a time series $x(s)$ are calculated using a simple convolution (Chao and Naito, 1995):

$$W_\psi(a,b) = \left(\frac{1}{a}\right)\int x(s)\psi\left(\frac{s-b}{a}\right)ds \quad (2)$$

where is Ψ the mother wavelet; the variable a is the scale factor that determines the characteristic frequency or wavelength; and b represents the shift of the wavelet over $x(s)$. We scaled the wavelet coefficient by $1/a$, which represents wavelet amplitudes, while most other applications use $1/\sqrt{a}$ to calculate the modulus or variance of the signals (Chao and Naito, 1995). The wavelet coefficients W are normalized to represent the amplitudes of Fourier frequencies. We have utilized a continuous wavelet transform (CWT), with the Morlet wavelet as the mother function (Morlet et al., 1982). The Morlet wavelet is simply a sinusoid with wavelength/period a modulated by a Gaussian function, which provides robust results in analyses of climate-related records (Prokoph and Barthelmes, 1996). A parameter l modifies wavelet transform bandwidth resolution either in favor of time or in favor of frequency, according to the uncertainty principle. The bandwidth resolution for wavelet transform varies with

$$\Delta a = \frac{a\sqrt{2}}{4\pi l} \quad (3)$$

and a location resolution

$$\Delta b = \frac{al}{\sqrt{2}.} \quad (4)$$

The parameter $l = N * \delta t = 10$ for all analyses is chosen in such a way that it gives sufficiently precise results in resolving depth and frequency, respectively (Prokoph and Barthelmes, 1996). The shifted and scaled Morlet mother wavelet is defined as (Morlet et al., 1982):

$$\Psi^l_{a,b}(s) = \pi^{-\frac{1}{4}}(al)^{-\frac{1}{2}}e^{-i2\pi\frac{1}{a}(s-b)}e^{-\frac{1}{2}\left(\frac{s-b}{al}\right)^2}. \quad (5)$$

The wavelet coefficients at the start and at the end of the time series are subject to 'edge effects' (Torrence and Compo, 1998).

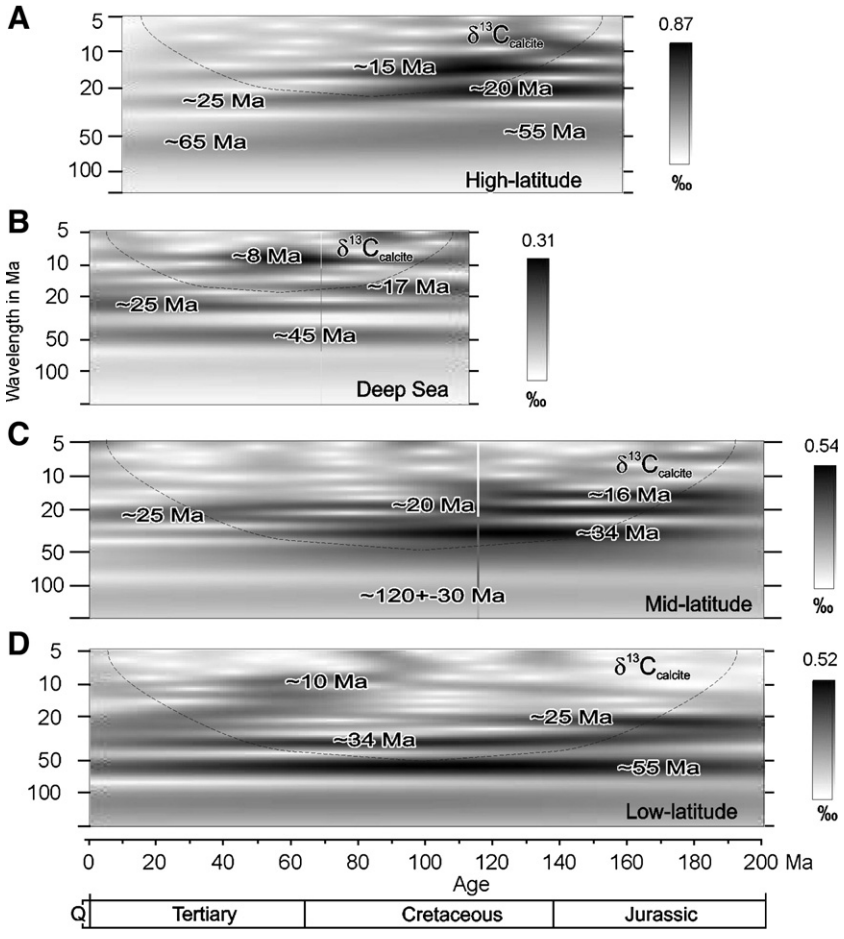

Fig. 15. Scalograms of wavelet transform for brachiopod-corrected $\delta^{13}C$ records for different habitats for the last 200 Ma. Area below dashed lines has >20% wavelet coefficient reduction due to edge effect. Right side: grey-scale code for wavelet coefficient above zero (white). Note that the highest wavelet coefficients appear in wavebands from 8 to 55 Ma.

For long wavelengths the edge effect can stretch across the entire time series. Thus, the boundary of edge effects on the wavelet coefficients is wavelength dependent forming the 'cone of (edge effect) influence' (Torrence and Compo, 1998). We displayed significant periodic signals after correction for edge effects. Details of the wavelet analysis algorithms used are provided in Prokoph and Barthelmes (1996).

6. Results

6.1. Oxygen and carbon isotope variability over the last 200 Ma

All carbon and oxygen isotope records have a data density of $p>0.25$ for at least 90% of the 1 Ma-intervals for the last 115 Ma, with the exception of the "high-latitude" $\delta^{13}C$ record.

The brachiopod-calibrated $\delta^{18}O$ results from all habitats show a negative trend with a slope of −0.0145‰/Ma for the "low-latitude" realm to −0.036‰/Ma for the "deep-sea" realm (Fig. 10). Note that the "high-latitude" record is well correlated with the "deep-sea" record.

The brachiopod-calibrated $\delta^{13}C$ records of the last 200 Ma do not show any significant linear trend (Fig. 11). The statistical offsets of the "low-latitude" realm relative to the "mid-latitude" and "deep-sea" ones have remained relatively stable throughout the last 115 Ma, at ~2‰ and 3‰, respectively. For the Early Cretaceous and Jurassic, the "low-" and "mid-latitude" $\delta^{13}C$ records are statistically indistinguishable at present. The data density for the entire "high-latitude" dataset is too sparse for calibration to brachiopods. Note, however, the similarity between the Tertiary planktic foraminifera from the "high-latitudes" and the benthic foraminifera from the "deep-sea" sets (Fig. 11).

Spectral analysis of the $\delta^{18}O$ record, after removal of the linear trend, shows that its >5 Ma variability is dominated by a 38±8 Ma cycle that is superimposed on a weak long-term cycle (Fig. 12A) that spans essentially the entire studied time interval

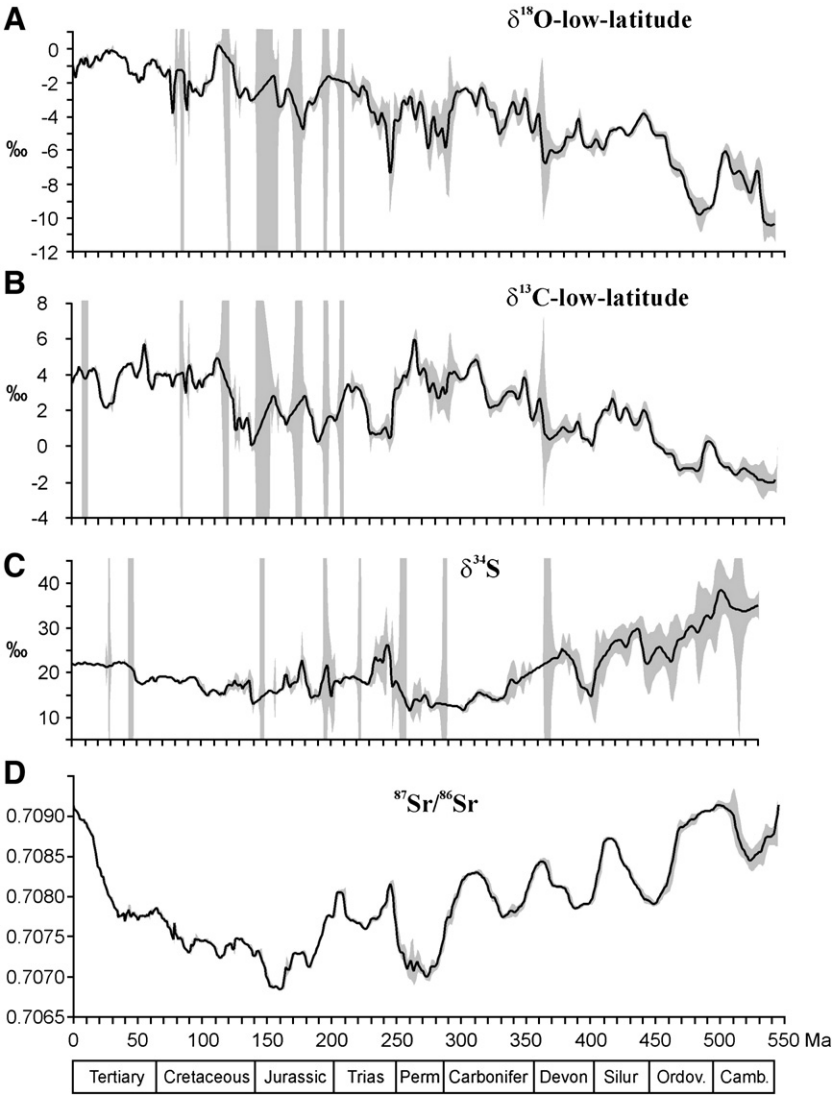

Fig. 16. Gaussian-filtered Phanerozoic isotope records: (A) "low-latitude" brachiopod-corrected $\delta^{18}O$ record, The $\delta^{18}O$ unidirectional linear trend of decreasing values with age is defined as $y=-0.0107t(\text{Ma})-0.7438(\text{Ma})$; (B) "mid-latitude" brachiopod-corrected $\delta^{13}C$ record; (C) $\delta^{34}S$ record; (D) $^{87}Sr/^{86}Sr$ record: 1 Ma intervals with $p<0.25$ are replaced by interpolated values. Grey shaded areas mark ±standard error of the mean for each 1 Ma-interval. Time-scale GTS2004 (Gradstein et al., 2004).

and is therefore of limited validity for statistical evaluation. These two cycles combined can explain >60% of the total variability in this isotope record, except for the "low-latitude" realm where they explain only ~32%. The ~38 Ma cycle alone accounts for 2/3 of the explained variability and is in phase in all habitat records (Fig. 12B). By contrast, there is no consistent periodicity in all $\delta^{13}C$ habitat records (Fig. 12C). In particular, the "deep-sea" realm shows only white noise.

Wavelet analysis of oxygen isotope data confirms that over the last 200 Ma all habitat records exhibit a ~38±8 Ma quasi-cyclicity (Fig. 13). As already pointed out (Fig. 12A) the apparent ~120±30 Ma frequency represents only a single cycle, insufficient for further contemplation. An additional ~9 Ma cyclicity appears in the "high-latitude" set during the Neogene and in the "low-latitudes" during the Cretaceous (Fig. 13). The 38±8 Ma cycle is at its shortest during the Tertiary, at ~33 Ma wavelength, and longest in the early Cretaceous.

The similarity of $\delta^{18}O$ in the "high-latitude" and "deep-sea" records (Fig. 10), with an intercept on today's axis of only 0.4‰ (based on the 115 Ma declining secular trend), implies only a small temperature difference of <2 °C, or a small salinity/pH contrast, between these two water masses. This indicates that, as in the Quaternary, the high-latitude surface waters could have been a source of deep-water masses since at least 115 Ma ago. The increasing difference in $\delta^{18}O$ between "deep-sea" and "high-latitude" vs. "low-latitude" water masses, from the Mid-Cretaceous onwards, has been recognized already by Savin (1977), and our results tentatively suggest that the gradient may have already existed earlier (Fig. 10).

A commonly cited estimate suggests a $\delta^{18}O_{seawater}$ of −1‰ (SMOW) as the pre-Oligocene ocean water value due to the absence of polar ice caps (Shackleton and Kennett, 1975). More recent estimates put this "ice-free ocean" value at −1.4‰ (Lhomme et al., 2005). Conversion of the $\delta^{18}O$ spectrum for the last 115 Ma into paleotemperature (Fig. 14) shows that the amplitudes of the ~38 Ma cycle in all habitats are larger than could be explained by glacial dynamics in the absence of significant ice caps. This amplitude, ~1.8‰ in "low-latitudes" and ~3‰ in all other realms, must therefore at least partially reflect changes in seawater temperature, pH or salinity (Zeebe, 2001; Royer et al., 2004), or a combination of these factors.

In concert with the spectral analysis, the wavelet analysis of the carbon isotope data shows that no distinctive cycle band dominates the latitudinal records of the last 200 Ma (Fig. 15). In particular, high frequency ~8–35 Ma cycles occur at different times in the different records. The longer, ~45–65 Ma, cycle band in most records has a maximum amplitude of ~0.5‰ in the "low-latitudes". Note, however, that the offset in $\delta^{13}C$ between deep and surficial habitats (Fig. 11) is consistent with operation of the biological pump (Sigman and Haugh, 2006) since at least the Cretaceous.

6.2. Variability in strontium, sulfur and "low-latitude" oxygen and carbon isotope records during the last 542 Ma

The strontium isotope record is stratigraphically the most complete and robust. This is expressed by a generally small standard error on the mean value for each 1 Ma interval (Fig. 16). The late Permian and the early Cambrian are the only time intervals with increased uncertainties of the mean values.

By contrast, the "low-latitude" $\delta^{18}O$ and $\delta^{13}C$ records have low data density and/or high variability on a million-year scale during the Turonian (~85–93 Ma), Aptian (~115–124 Ma), several Jurassic intervals and during the late Triassic. This is expressed by extremely high standard errors on the estimates of the mean values (Fig. 16A and B). The $\delta^{13}C$ values for the Mid-Miocene (~13–9 Ma) are also sparse. Both sets, $\delta^{13}C$ and $\delta^{18}O$, also have low data density and/or high variability for the early Permian (~290 Ma), the late Devonian (~360 Ma) and an increasing noise level for the Early–Mid-Cambrian.

The sulfur isotope record shows fluctuating data density throughout the Phanerozoic with particularly low resolution during the Cambrian–Devonian, Late Permian–Early Triassic and early Jurassic time intervals (Fig. 17C).

The $\delta^{18}O$ record is the only record with a significant ($R^2=0.69$) linear trend through the Phanerozoic, with a gradient, close to the regression for the last 115 Ma (Fig. 10). By contrast, carbon, sulfur and strontium isotope records show no significant unidirectional long-term trends.

Spectral analyses of the isotope records of the last 543 Ma show that most of the variance occurs in wavelengths >30 Ma (Fig. 17). None of these cycles has significant coherency with other isotopes throughout the entire Phanerozoic. The 90–150 Ma cycle in the $\delta^{18}O$ record is the most significant multi-million year signal and by itself explains ~25% of the total variance of oxygen isotopes.

Wavelet analysis shows that most Phanerozoic cyclicity occurs at different time intervals in all records (Fig. 18). Note,

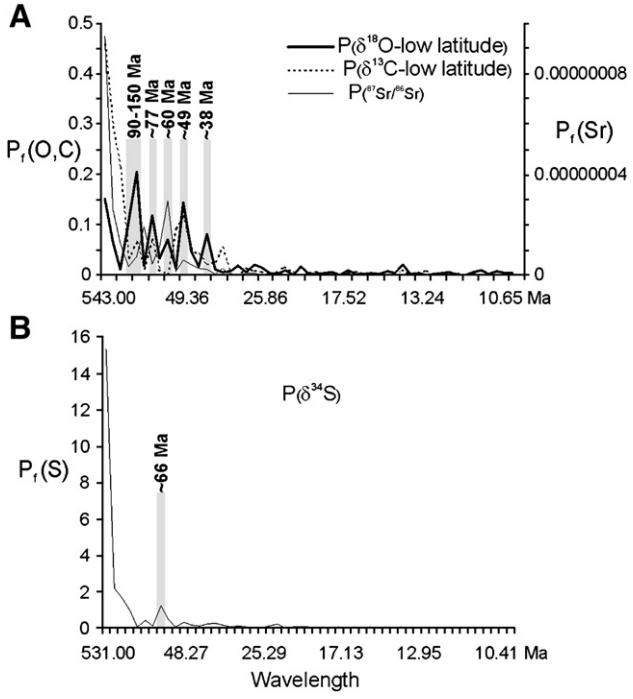

Fig. 17. Spectral analysis: (A) $^{87}Sr/^{86}Sr$ and brachiopod-corrected "low-latitude" $\delta^{18}O$ and $\delta^{13}C$ records for the last 543 Ma; (B) $\delta^{34}S$ record for the last 531 Ma. Note that the $\delta^{18}O$ signal is detrended.

however, that the highest amplitude wavelengths in the $\delta^{13}C$ and δ^{34} S records covary (Fig. 19A) in response to the redox controlled coupling of the carbon and sulfur cycles (Garrels and Perry, 1974; Holland, 2006) that results in negative correlation of their marine isotope records (Veizer et al., 1980; Veizer and Mackenzie, 2006). The highest amplitudes of the cycle bands decrease through time for the S, O and C isotope records, but increase for the Strontium isotope record (Fig. 19B).

6.3. Long-term trends and cycles in strontium, oxygen and carbon isotope records through the last 3500 Ma

The corrected $\delta^{13}C$ and $\delta^{18}O$ whole rock records are plotted in Fig. 20. The significant negative trend found in the Phanerozoic fossil $\delta^{18}O$ data continues in the Precambrian whole rock record, but at a much lower slope. The projection of this slope would result in the present average $\delta^{18}O$ for calcite in equilibrium with seawater of −5.75‰ vs. PDB.

Wavelet analysis shows that both records, oxygen and carbon, exhibit ~900 Ma and ~400/450 Ma (Fig. 21B–C) quasi-cyclicity.

7. General remarks on the limits of the database

The database presented here is the most comprehensive marine isotope dataset to date that spans the entire Earth's history up to about 3700 Ma. The selection of data for the database followed previously proposed criteria (Veizer et al., 1999; Shields and Veizer, 2002) in the hope that the selected data will prove useful for interpretations of the evolution of Earth's surface environment, including paleoclimate and the geologic carbon cycle. For shorter time-scales and/or regional studies we refer to other databases that are commonly of higher resolution, and have even stricter criteria for data inclusion (e.g., Stoll and Schrag, 2000; Zachos et al., 2001; Lisiecki and Raymo, 2005; Ravizza and Zachos, 2006). Despite the massive

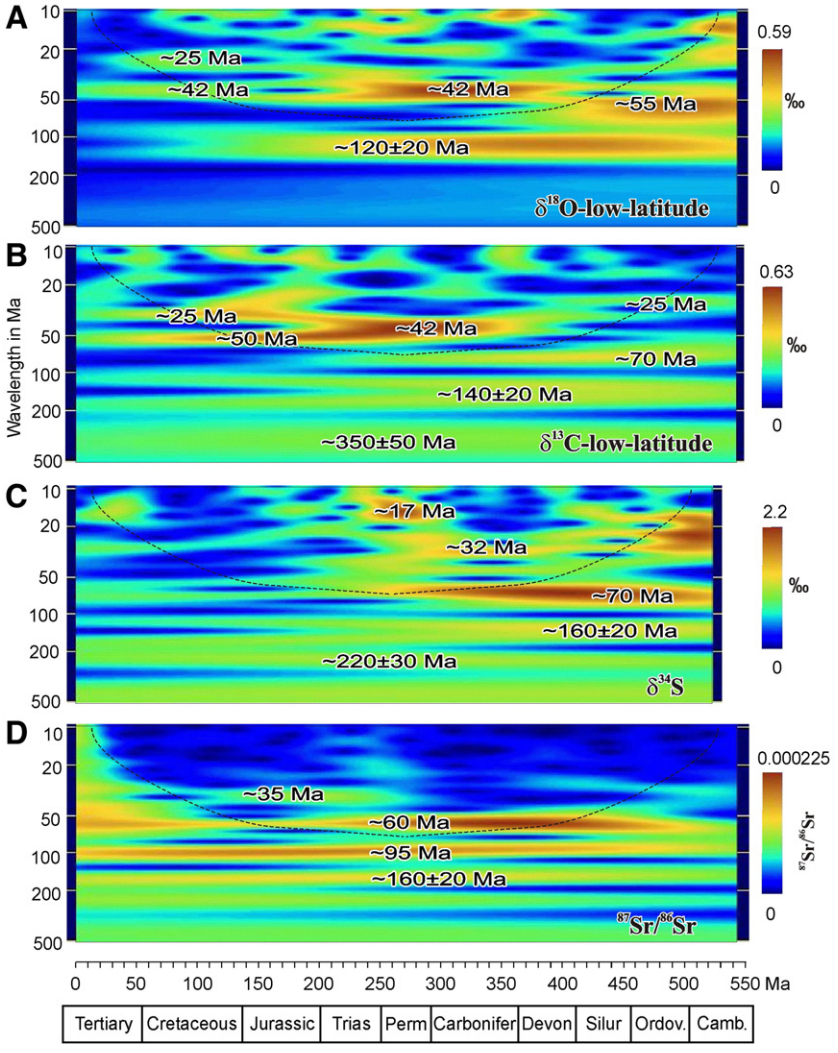

Fig. 18. Scalograms of wavelet transform for the $^{87}Sr/^{86}Sr$, $\delta^{34}S$, and the brachiopod-corrected "low-latitude" $\delta^{18}O$ and $\delta^{13}C$ records for the last 543 Ma. Area below dashed lines has >20% wavelet coefficient reduction due to edge effect. Right side: color-scale code for wavelet coefficient above zero (white). Note that the $\delta^{18}O$ signal is detrended.

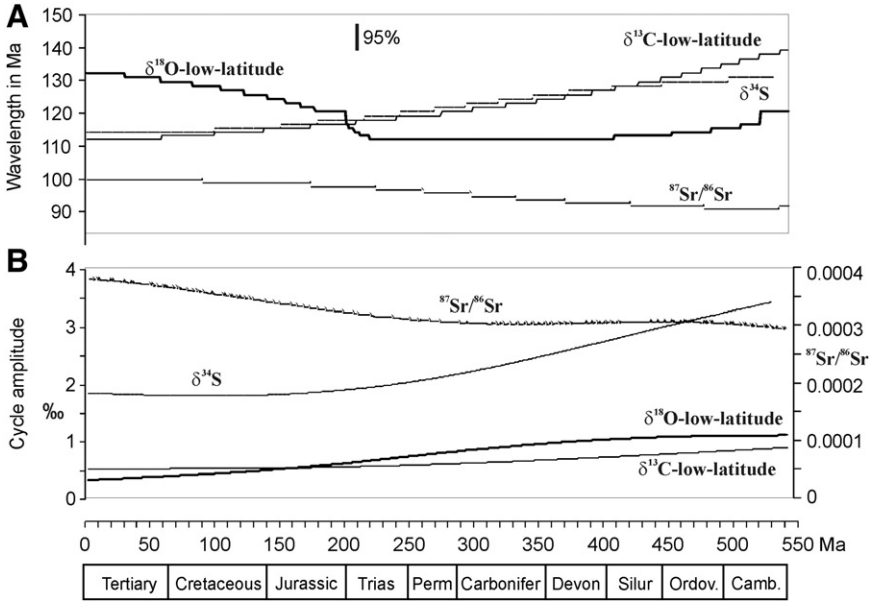

Fig. 19. Detailed results of wavelet analysis for the last 543 Ma: A: Highest-amplitude wavelength for different isotope records through time (see also Fig. 18). B: Edge effect-corrected amplitudes of wavelengths. Time-scale GTS2004 (Gradstein et al., 2004).

database (~39,000 Phanerozoic fossil and ~16,500 whole rock measurements), its resolution and consistency varies for different time intervals and isotopic systems. Our processing stream from raw sample data to concise global records uses only simple algebra and repeatable and reproducible methods. Statistical estimates, such as mean values, standard errors, confidence intervals and standard deviations are used only sparsely, in order to highlight major features for further interpretation, not as parameters for further processing.

The results of time-series analysis are presented without significance intervals in order to avoid any impression that they can obviate the need for high-quality, stratigraphically continuously sampled data, particularly of brachiopods. Nevertheless, the database is of sufficient size and quality that it

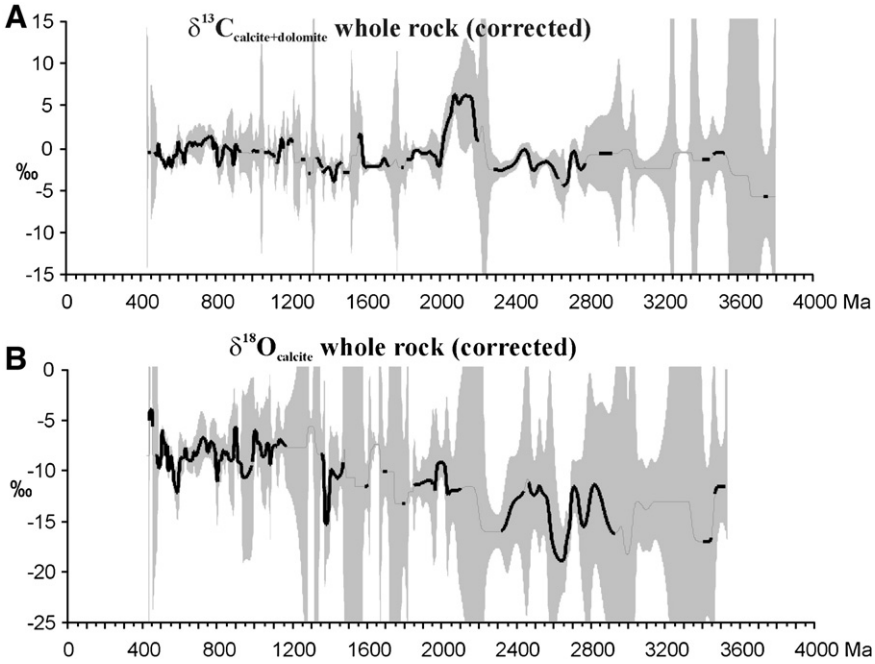

Fig. 20. Whole rock carbon isotope (A), and oxygen (B) data through the Earth's history, Gaussian filtered, corrected, but not detrended. Data with $p > 0.1$ are plotted as bold black line, grey shaded area marks the standard error of the mean.

enables paleoenvironmental interpretations at higher temporal and spatial resolution than previously possible (e.g., Shaviv and Veizer, 2003).

The Phanerozoic marine $^{87}Sr/^{86}Sr$ database has been only slightly enhanced and corrected from previous versions (Veizer et al., 1999; Shields and Veizer, 2002). This database is robust with relatively low uncertainty to the mean values, with the exception of the Permian and Cambrian records. The Sr record in particular can be utilized for stratigraphic refinements at resolutions of up to 2 Ma (McArthur et al., 2004). In contrast, the Precambrian strontium isotope database needs additional, stratigraphically more evenly distributed, and diagenetically little altered samples before it will be amenable to statistical treatment. The most important outstanding issue is the veracity of the early Archean record, with $^{87}Sr/^{86}Sr$ values more radiogenic than the coeval mantle (Fig. 8). The preferred interpretation today is that this shift to higher values is a consequence of post-depositional alteration. Should this not be the case, and the data prove representative of coeval seawater, a greater role for ancient continental crust has to be anticipated than is presently envisaged.

8. Discussion

Trend, correlation, wavelet, and spectral analysis have been applied to detect and quantify similarities and patterns in all records.

Oxygen isotope trends for the "high-latitude" and "deep sea" are almost identical during at least the last 115 Ma, i.e. roughly since the Aptian–Albian boundary of the late Early Cretaceous, albeit punctuated by short warmer intervals with apparent cyclicity of about 38 Ma. This suggests continuous operation of the "conveyor belt" during this entire interval, with sinking high-latitude surface water replenishing the deep-water reservoir. As warmer water holds less oxygen than cold water, a small latitudinal temperature gradient, as during mid-Cretaceous times (Huber et al., 1995), may have led to dysoxic deep-water conditions and thus greater opportunity for oceanic black shale formation. The strong 30–45 Ma (~38 Ma) cyclicity in all oxygen isotope habitat records could thus be coincident with the occurrence of oceanic anoxic sediments throughout the Cretaceous and Cenozoic, and potentially also the entire Mesozoic (Prokoph et al., 2004). Note also that the good fit between "high-latitude" and "deep-sea" datasets may help in construction of longer records when stratigraphically older, high-latitude planktic foraminifera or brachiopod data become available.

Up to 70% of the multi-million year variability in the $\delta^{18}O$ record for the last 115 Ma, and potentially Earth's climate, can be modeled by the following approximation

$$\delta^{18}O(‰) = 0.6\sin(2\pi t/120\ \text{Ma} + 0.9) + X\sin(2\pi t/38.3\ \text{Ma} + 1.1)$$

with X ranging from 0.4–0.6‰ for the "low-", "high-latitude ", and "deep sea" and up to 0.8‰ for the "mid-latitude" realms, the latter experiencing the most pronounced oxygen isotope fluctuations. For the Phanerozoic, the previously indicated cyclicity of ~140 Ma (Veizer et al., 2000; Shaviv and Veizer, 2003) falls

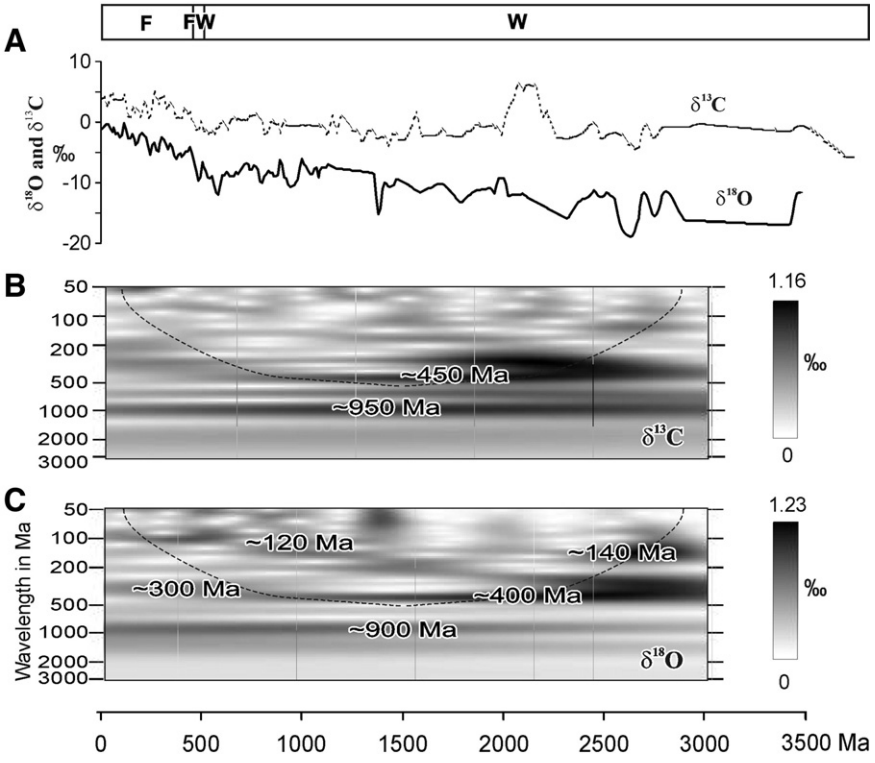

Fig. 21. (A) Corrected and combined fossil and whole rock isotope records through Earth's history. F and W represent the range of data based on fossils and whole rocks, respectively. (B) Scalograms of wavelet transform $\delta^{13}C$ isotope record. (C) Scalogram for ABS corrected and detrended $\delta^{18}O$. Area below dashed lines has >20% wavelet coefficient reduction due to edge effect. Right side: grey-scale code for wavelet coefficient.

within a broad bandwidth of 90–150 Ma (Fig. 17). The causes of this "four-hump" cyclic pattern (Fig. 22), have been discussed widely (Veizer et al., 2000; Crowley and Berner, 2001; Shaviv and Veizer, 2003; Royer et al., 2004) as potentially reflecting galactic orbital modulation of climate (Shaviv, 2003) due to the impact of cosmic rays on cloud cover (e.g., Carslaw et al., 2002), climate modulation due to variable atmospheric CO_2 concentrations (Berner and Kothavala, 2001), and related impact on seawater pH (Royer et al., 2004), or a combination of these causes (Wallmann, 2004). The putative carbon and oxygen isotope cyclicities at ~450 and ~900 Ma require further verification. At this stage, we are unaware of a potential geologic and/or extraterrestrial phenomena that could cause such oscillations.

The present Phanerozoic database and time-series analysis yields results comparable to earlier studies (Veizer et al., 1999), despite utilization of the most recent geologic time scale (Gradstein et al., 2004). Only the disputed Jurassic pattern has now a weaker amplitude and greater uncertainties (Fig. 22B), arguing for a relatively warm coeval climate inconsistent with paleoclimate reconstructions based on climatically sensitive sediments, CO_2 proxies, and fossils (Fig. 22 A,C,E). It is possible that the downward shift in $\delta^{18}O$ results mostly from the

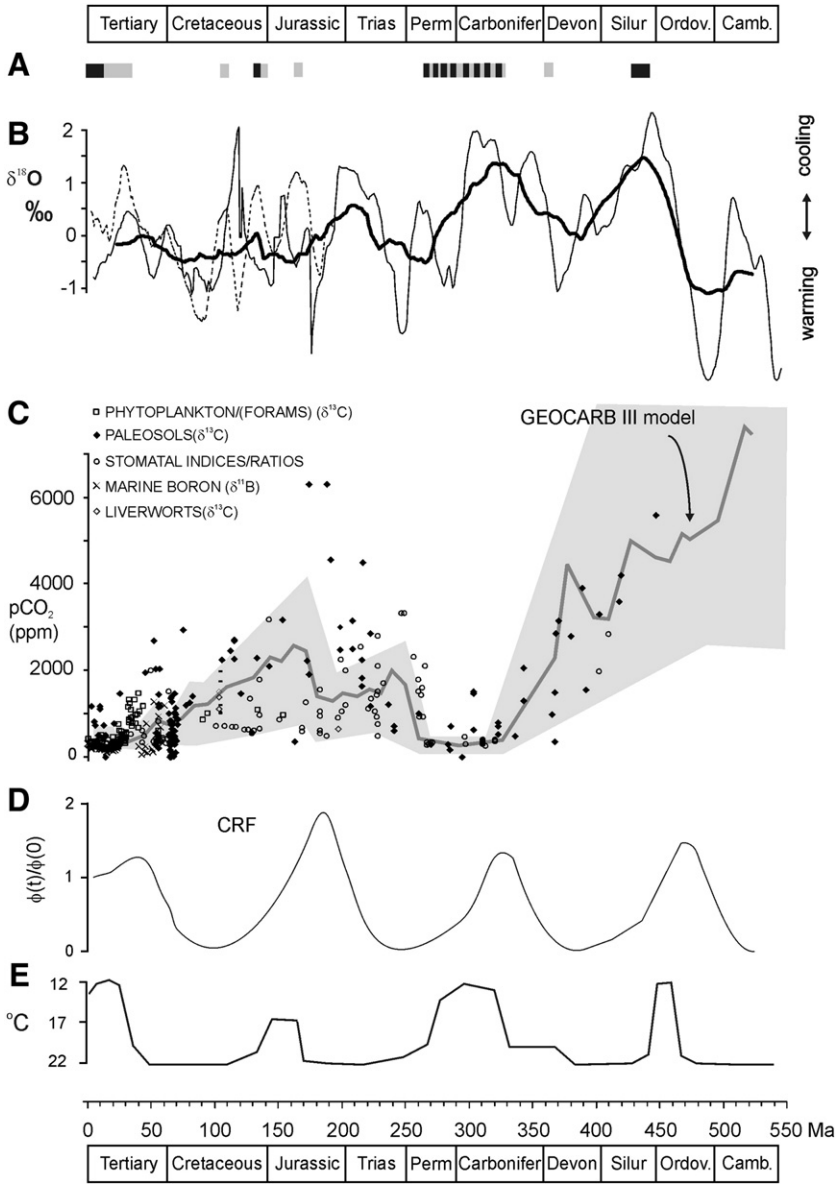

Fig. 22. Phanerozoic climate history. A: Evidence for ice-sheets or ice-transported marine drift as black and grey shading, respectively (Kemper, 1987; Frakes and Francis, 1988; Price, 1999; Dromart et al., 2003; Isbell et al., 2003; Alley and Frakes, 2003; Jones and Fielding, 2004; Fielding et al., 2006). B: $\delta^{18}O$ record. The data are Gaussian filtered with $\pm 1\sigma$ uncertainty (dashed lines) and the linear secular trend has been removed. The bold line marks the 1/50 Ma moving average of the "low-latitude" data, the thin solid line marks the 1/10 Ma moving average of "low-latitude" data, and the dashed line marks the 1/10 Ma moving average of the "mid-latitude" data. C: CO_2 proxy data (mean values) compiled by Royer (2006), and the estimated atmospheric CO_2 ranges for the GEOCARB III model (Berner and Kothavala, 2001). Shaded area marks the uncertainties of the CO_2 model. D: normalized cosmic ray flux (Shaviv and Veizer, 2003); E: Paleoclimate interpretation based on the paleogeographic distribution of climate sensitive sediments and fossils (www.scotese.com/climate.htm; Fig. 1 in Boucot and Gray, 2001).

smoothing effect of the 50 Ma window, since the trends based on the 10 Ma window show more positive $\delta^{18}O$ pathways. Note also that this portion of the database is based mostly on belemnites, with the large offset corrections applied to these data (Table 2). As stated earlier, the offset is based on studies of a low-latitude sequence in Spain (Rosales et al., 2001, 2004) and may not be a definitive correction. For example, the $\delta^{18}O$ data on brachiopods and belemnites in the "mid-latitude" realm (Wierzbowski, 2002) are similar, suggesting that they occupied the same water mass and, if so, the correction would not be applicable, resulting in a cooler ocean. Moreover, belemnite species may have had different habitats. At present, some species of the related family of squids (e.g., Humboldt squid) migrate each year over long distances, at 200–700 m water depth, while other species live in the surface water layer and do not migrate. In general, the isotopic difference between belemnites and brachiopods is large and variable and may also be species specific. At this stage, we accept the validity of the offset, but point out that high-quality coeval brachiopod/belemnite isotope results are rare, subject to local environmental and diagenetic influences, and that more definitive data are required to confirm the global validity of the proposed correction.

In contrast to oxygen, the carbon isotope record shows different frequency patterns, and trends and the patterns for different habitats do not correlate. The exceptions may be the peaks in the Aptian and the Paleogene, and the Oligocene depression (Fig. 11). Oxygen and carbon isotopes have significant coexisting ~42–55 Ma cyclicity only from the Permian to the Jurassic (Fig. 18A,B), and not during the entire Phanerozoic. Thus, the stable isotope record, as represented by published $\delta^{13}C_{carb}$ and $\delta^{18}O$ data, does not provide unambiguous support for a long-term relationship between the carbon cycle and paleoclimate. We are aware that much of the carbon isotope variability occurs over intervals shorter than 1 Ma, not resolvable in this study. Such higher resolution studies may be more suitable for studies of the linkage between climate and carbon cycles.

Acknowledgements

We thank the Natural Science and Engineering Research Council of Canada (NSERC) and the Canadian Institute for Advanced Research (Noranda, G.G. Hatch) for the financial support. G.A. Shields gratefully acknowledges the financial support of the Alexander von Humboldt Foundation during 2006 and 2007.

Appendix A. Supplementary data

Supplementary data associated with this article can be found, in the online version, at doi:10.1016/j.earscirev.2007.12.003.

References

Abramovitch, S., Keller, G., Stueben, D., Berner, Z., 2003. Characterization of Late Campanian and Maastrichtian planktonic foraminiferal depth habitats and vital activities based on stable isotopes. Palaeogeography, Palaeoclimatology, Palaeoecology 202, 1–29.

Agterberg, F.P., 1994. Estimation of the geological time scale. Mathematical Geology 26, 857–876.

Alley, N.F., Frakes, L.A., 2003. First known Cretaceous glaciation: livingstone tillite member of the Cadnaowie Formation, South Australia. Australian Journal. Earth Science 50 (2), 139–144.

Berner, R.A., Kothavala, Z., 2001. GEOCARB III: a revised model of atmospheric CO_2 over Phanerozoic time. American Journal of Science 301, 18–204.

Boucot, A.J., Gray, J., 2001. A critique of Phanerozoic climatic modes involving changes in the CO_2 content of the atmosphere. Earth Science Reviews 56, 1–159.

Brand, U., 2004. Carbon, oxygen and strontium isotopes in Paleozoic carbonate components: an evaluation of original seawater-chemistry proxies. Chemical Geology 204, 23–44.

Canfield, D.E., Raiswell, R., 1999. The evolution of the sulfur cycle. American Journal of Science 299, 697–729.

Carslaw, K.S., Harrison, R.G., Kirkby, J., 2002. Cosmic rays, clouds, and climate. Science 298, 1732–1737.

Chao, B.F., Naito, I., 1995. Wavelet analysis provides a new tool for studying Earth's rotation. EOS 76, 161, 164–165.

Corfield, R.M., Hall, M.A., Brasier, M.D., 1990. Stable isotope evidence for foraminiferal habitats during the development of the Cenomanian/Turonian oceanic anoxic event. Geology 18, 175–178.

Courtillot, V.E., Renne, P.R., 2003. On the ages of flood basalt events. Comptes Rendus Geoscience 335, 113–140.

Crowley, T.J., Berner, R.A., 2001. CO_2 and climate change. Science 292, 870–872.

Davis, J.C., 1986. Statistics and Data Analysis in Geology. Wiley, New York.

Dromart, G., Garcia, J.-P., Picard, S., Atrops, F., Lecuyer, C., Sheppard, S.M.F., 2003. Ice age at the Middle–Late Jurassic transition? Earth and Planetary Science Letters 213, 205–220.

Faure, G., 1998. Principles and Applications of Geochemistry. Prentice Hall, New Jersey.

Fielding, C.R., Rygel, M.C., Frank, T.D., Birgenheier, L.P., Jones, A.T., Roberts, J., 2006. Near-field stratigraphic record of the Late Paleozoic Gondwanan Ice Age from Eastern Australia Discloses multiple, alternating glacial and non-glacial intervals. 2006 Philadelphia Annual Meeting (22–25 October 2006), Geological Society of America, Abstract with Programs 38 (7), p. 137.

Frakes, L.A., Francis, J.E., 1988. A guide to Phanerozoic cold polar climates from high-latitude ice rafting in the Cretaceous. Nature 333, 547–549.

Garrels, R.M., Perry Jr., E.C., 1974. Cycling of carbon, sulfur and oxygen through geologic time. In: Golberg, E.D. (Ed.), The Sea, vol. 5. Wiley, New York, pp. 303–336.

Gradstein, F., Ogg, J., Smith, A., 2004. A Geologic Time Scale 2004. Cambridge Univ. Press, Cambridge, U.K.

Holland, H.D., 2006. The geologic history of seawater. In: Elderfield, H. (Ed.), Treatise on Geochemistry, vol. 6. Elsevier, Amsterdam, pp. 583–625.

Huber, B.T., Hodell, D.A., Hamilton, C.P., 1995. Middle-late Cretaceous climate of the southern high latitudes; stable isotopic evidence for minimal equator-to-pole thermal gradients. Geological Society of America Bulletin 107, 1164–1191.

Isbell, J.L., Lenaker, P.A., Askin, R.A., Miller, M.F., Babcock, L.E., 2003. Reevaluation of the timing and extent of late Paleozoic glaciation in Gondwana: role of the Transantarctic Mountains. Geology 31, 977–980.

Jaffrés, J.B.D., 2005. Development of a model to evaluate seawater oxygen isotope evolution over the last 3.4 billion years. B.Sc. Thesis, James Cook University, Townsville, Australia.

Jaffrés, J., Shields, G.A., Wallmann, K., 2007. The oxygen isotope evolution of seawater: a critical review of a long-standing controversy and an improved geological water cycle model for the past 3.4 billion years. Earth Science Reviews 83, 83–122.

Jones, A.T., Fielding, C.R., 2004. Sedimentological record of the late Paleozoic glaciation in Queensland, Australia. Geology 32, 153–156.

Kampschulte, A., Strauss, H., 2004. The sulfur isotopic evolution of Phanerozoic seawater based on the analysis of structurally substituted sulfate in carbonates. Chemical Geology 204, 255–286.

Keith, M.L., Weber, J.N., 1964. Carbon and oxygen isotopic composition of selected limestones and fossils. Geochim. Cosmochim. Acta 28, 1787–1816.

Kemper, E., 1987. Das Klima der Kreidezeit. Geologisches Jahrbuch A96, 5–185.

Lhomme, N., Clarke, G.K.C., Ritz, C., 2005. Global budget of water isotopes inferred from polar ice sheets. Geophysical Research Letters 32, L20502. doi:10.1029/2005GL023774.

Lisiecki, L.E., Raymo, M.E., 2005. A Pliocene–Pleistocene stack of 57 globally distributed benthic $\delta^{18}O$ records. Paleoceanography 20, 1–17 PA1003.

Lu, G., Keller, G., 1996. Separating ecological assemblages using stable isotope signals. Late Paleocene to early Eocene planktic foraminifera, DSDP site 577. Journal of Foraminiferal Research 26, 103–112.

McArthur, J.M., Donovan, D.T., Thirwall, M.F., Fouke, B.W., Mattey, D., 2000. Strontium isotope profile of the early Toarcian (Jurassic) oceanic anoxic event, the duration of ammonite biozones, and belemnite palaeotemperatures. Earth and Planetary Science Letters 179, 269–285.

McArthur, J.M., Mutterlose, J., Price, G.D., Rawson, P.F., Ruffell, A., Thirlwall, M.F., 2004. Belemnites of Valanginian, Hauterivian and Barremian age: Sr–isotope stratigraphy, composition ($^{87}Sr/^{86}Sr$, $\delta^{13}C$, $\delta^{18}O$, Na, Sr, Mg) and palaeoceanography. Palaeogeography, Palaeoclimatology, Palaeoecology 202, 253–272.

Morlet, J., Arehs, G., Fourgeau, I., Giard, D., 1982. Wave propagation and sampling theory. Geophysics 47, 203.

Pearson, P.N., Ditchfield, P.W., Singano, J., Harcourt-Brown, K.G., Nicholas, C.J., Olsson, R.K., Shackleton, N.J., Hall, M.A., 2001. Warm tropical sea surface temperatures in the Late Cretaceous and Eocene epochs. Nature 413, 481–487.

Peterman, Z.E., Hedge, C.E., Tourtelot, M.A., 1970. Isotopic composition of strontium in seawater throughout the Phanerozoic. Geochimica et Cosmochimica Acta 34, 105–120.

Picard, S., Garcia, J.-P., Lecuyer, C., Sheppard, S.M.F., Cappetta, H., Emig, C.C., 1998. $\delta^{18}O$ values of coexisting brachiopods and fish: temperature differences and estimates of paleo-water depths. Geology 26, 975–978.

Price, G.D., 1999. The evidence and implications of polar ice during the Mesozoic. Earth-Science Reviews 48, 183–210.

Prokoph, A., Barthelmes, F., 1996. Detection of nonstationarities in geologic time series: wavelet transform of chaotic and cyclic sequences. Computer & Geoscience 22, 1097–1108.

Prokoph, A., Rampino, M.R., El Bilali, H., 2004. Periodic components in the diversity of calcareous plankton and geologic events over the past 230 Ma. Palaeogeography, Palaeoclimatology, Palaeoecology 207, 105–125.

Ravizza, G.E., Zachos, J.C., 2006. Records of Cenozoic ocean chemistry. In: Elderfield, H. (Ed.), Treatise on Geochemistry, vol. 6. Elsevier, Amsterdam, pp. 551–581.

Rosales, I., Queseda, S., Robles, S., 2001. Primary and diagenetic isotopic signals in fossils and hemipelagic carbonates: the Lower Jurassic of northern Spain. Sedimentology 48, 1149–1169.

Rosales, I., Queseda, S., Robles, S., 2004. Paleotemperature variations of Early Jurassic seawater recorded in geochemical trends of belemnites from the Basque–Cantabrian basin, northern Spain. Palaeogeography, Palaeoclimatology, Palaeoecology 203, 253–275.

Royer, D.L., Berner, R.A., Montanez, I.P., Tabor, N.J., Beerling, D.J., 2004. CO_2 as a primary driver of Phanerozoic climate. GSA Today 3, 4–10.

Royer, D.L., 2006. CO_2-forced climate thresholds during the Phanerozoic. Geochimica et Cosmochimica Acta 70, 5665–5675.

Savin, S.M., 1977. The history of the Earth's surface temperature during the past 100 million years. Annual Review of Earth and Planetary Science 5, 319–355.

Shackleton, N.J., Imbrie, J., 1990. The $\delta^{18}O$ spectrum of oceanic deep water over a five-decade band. Climate Change 16, 217–230.

Shackleton, N.J., Kenneth, J.P., 1975. Paleotemperature history of the Cenozoic and initiation of Antarctic glaciation. oxygen and carbon isotope analysis in DSDP sites 277, 279 and 281. In: Kenneth, J.P., Houtz, R.E. (Eds.), Initial reports of the deep sea drilling project, Volume 29, pp. 743–755.

Shaviv, N.J., 2003. The spiral structure of the milky way, cosmic-rays and ice-age epochs on Earth. New Astronomy 8, 39–77.

Shaviv, N.J., Veizer, J., 2003. Celestial driver of Phanerozoic climate? GSA Today 13, 4–10.

Shields, G., Veizer, J., 2002. Precambrian marine carbonate isotope database: version 1.1. Geochemistry, Geophysics, Geosystems 3 (6) June 6, 12 pp. (http://g-cubed.org/gc2002/2001GC000266).

Sigman, D.M., Haug, G.H., 2006. The biological pump in the past. In: Elderfield, H. (Ed.), Treatise on Geochemistry, vol. 6. Elsevier, Amsterdam, pp. 491–528.

Spero, H.J., DeNiro, M.J., 1987. The influence of symbiontic photosynthesis on the $\delta^{18}O$ and $\delta^{13}C$ values of foraminiferal shell calcite. Symbiosis 4, 213–228.

Spero, H.J., Bjima, J., Lea, D.W., Bemis, B.E., 1997. Effect of seawater carbonate concentration on foraminiferal carbon and oxygen isotopes. Nature 390, 497–500.

Stoll, H.M., Schrag, D.P., 2000. High-resolution stable isotope records from the Upper Cretaceous rocks of Italy and Spain: glacial episodes in a greenhouse planet? GSA Bulletin 112, 308–319.

Strauss, H., 2002. The isotopic composition of Precambrian sulphides — seawater chemistry and biological evolution. Special publication of the International Association of Sedimentologists 33, 67–105.

Strauss, H., DesMarais, D.J., Hayes, J.M., Summons, R.E., 1992. The carbon isotope record. In: Schopf, J.W., Klein, C. (Eds.), The Proterozoic Biosphere. Cambridge Univ. Press, Cambridge, pp. 117–127.

Torrence, C., Compo, G.P., 1998. A practical guide to wavelet analysis. Bulletin American Meteorological Society 79, 61–78.

Veizer, J., Compston, W., 1974. $^{87}Sr/^{86}Sr$ composition of seawater during the Phanerocoic. Geochimica et Cosmochimica Acta 38, 1461–1484.

Veizer, J., Hoefs, J., 1976. The nature of O^{18}/O^{16} and C^{13}/C^{12} secular trends in sedimentary carbonate rocks. Geochimica et Cosmochimica Acta 40, 1387–1395.

Veizer, J., Mackenzie, F.T., 2004. Evolution of sedimentary rocks. In: Mackenzie, F.T. (Ed.), Treatise on Geochemistry, vol. 7. Elsevier, Amsterdam, pp. 369–407.

Veizer, J., Holser, W.T., Wilgus, C.K., 1980. Correlation of $^{13}C/^{12}C$ and $^{34}S/^{32}S$ secular variations. Geochimica et Cosmochimica Acta 44, 579–587.

Veizer, J., Ala, D., Azmy, K., Bruckschen, P., Buhl, D., Bruhn, F., Carden, G.A.F., Diener, A., Ebneth, S., Goddéris, Y., Jasper, T., Korte, C., Pawellek, F., Podlaha, O.G., Strauss, H., 1999. $^{87}Sr/^{86}Sr$, ^{13}C and ^{18}O evolution of Phanerozoic seawater. Chemical Geology 161, 59–88.

Veizer, J., Godderis, Y., François, L.M., 2000. Evidence for decoupling of atmospheric CO_2 and global climate during the Phanerozoic eon. Nature 408, 698–701.

Voigt, S., Wilmsen, M., Mortimore, R.N., Voigt, T., 2003. Cenomanian palaeotemperatures derived from the oxygen isotopic composition of brachiopods and belemnites. evaluation of Cretaceous palaeotemperature proxies. International Journal of Earth Sciences 92, 285–299.

Wallmann, K., 2004. Impact of atmospheric CO_2 and galactic cosmic radiation on Phanerozoic climate change and the marine $\delta^{18}O$ record. Geochemistry, Geophysics, Geosystems 5, Q06004. doi:10.1029/2003G000683.

Wierzbowski, H., 2002. Detailed oxygen and carbon isotope stratigraphy of the Oxfordian in Central Poland. International Journal of Earth Sciences 91, 304–314.

Zachos, J., Pagani, M., Sloan, L., Thomas, E., Billups, K., 2001. Trends, rhythms, and aberrations in global climate 65 Ma to present. Science 282, 686–693.

Zakharov, Y.D., Boriskina, N.G., Popov, A.M., 2001. The Reconstruction of Late Paleozoic and Mesozoic Marine Environments from Isotopic Data. Dalnauka, Vladivostok. 112 pp.

Zeebe, R.E., 2001. Seawater pH and isotopic paleotemperatures of Cretaceous oceans. Palaeogeography, Palaeoclimatology, Palaeoecology 122, 143–166.